Recent Advances in Flexible and Stretchable Bio-Electronic Devices Integrated with Nanomaterials

Suji Choi, Hyunjae Lee, Roozbeh Ghaffari, Taeghwan Hyeon, and Dae-Hyeong Kim*

Flexible and stretchable electronics and optoelectronics configured in soft, water resistant formats uniquely address seminal challenges in biomedicine. Over the past decade, there has been enormous progress in the materials, designs, and manufacturing processes for flexible/stretchable system subcomponents, including transistors, amplifiers, bio-sensors, actuators, light emitting diodes, photodetector arrays, photovoltaics, energy storage elements, and bare die integrated circuits. Nanomaterials prepared using top-down processing approaches and synthesis-based bottom-up methods have helped resolve the intrinsic mechanical mismatch between rigid/planar devices and soft/curvilinear biological structures, thereby enabling a broad range of non-invasive, minimally invasive, and implantable systems to address challenges in biomedicine. Integration of therapeutic functional nanomaterials with soft bioelectronics demonstrates therapeutics in combination with unconventional diagnostics capabilities. Recent advances in soft materials, devices, and integrated systems are reviews, with representative examples that highlight the utility of soft bioelectronics for advanced medical diagnostics and therapies.

1. Introduction

Rapid advances in the design of ultrathin electronic/optoelectronic devices, sensors[1–3] and actuators,[4,5] and soft biocompatible/bioresorbable encapsulating layers[6,7] have broadened the scope of flexible/stretchable electronics from foldable displays and curved solar panels to new classes of soft bioelectronics systems that interface with the complex geometries, curved surfaces, and time dynamic tissues of the human body.[8–10]

A wide range of biological signals, including electrophysiological (e.g., electroencephalogram (EEG), electrocardiogram (ECG)),[11,12] physiological (e.g., pulse, temperature),[13,14] thermal (e.g., thermal conductivity, temperature distribution),[14,15] mechanical (e.g., strain, pressure),[13,16] and biochemical (e.g., glucose, pH) information,[17,18] continuously emanate from the human body. Each of these signals contains important clinical cues about normal bodily functions and the manifestation and progression of various diseases.[19–21] There are significant challenges, however, in our ability to access target tissues/organs for high quality signal capture due to the rigid and bulky characteristics of conventional medical systems.

To achieve soft, stretchable bioelectronics requires novel approaches in material designs: i) strain minimization via nanoscale processing of established materials and ii) synthesis of new functional nanomaterials. Once bulk rigid materials are thinned and oriented into nano-structures, they become deformable. For example, the flexural rigidity of silicon nano-membranes (Si NMs) (≈2 nm) is fifteen orders of magnitude smaller than that of silicon (Si) wafers (≈200 μm).[22] A hybrid of top-down-processed nanomaterials and bottom-up-synthesized nanomaterials can create further multi-functionalities/high-performances without sacrificing the mechanical deformability. These chemically-synthesized nanomaterials exhibit unique electrical,[23,24] optical,[25,26] and electrochemical[27] properties that their bulk counterparts do not possess.

In the following, we summarize the recent state of the art in soft, flexible and stretchable electronics/optoelectronics being employed in biomedicine for implantable, minimally invasive, and wearable applications. We also present a brief introduction of nanostructured materials and related engineering technologies with emphasis on the nanometer-size designs for reliable performances under mechanical deformations. We then provide a detailed description of flexible and stretchable sensors and actuators for skin-mounted and implanted systems. Mechanically deformable optoelectronics, memory modules, and energy supply devices that consist of bioelectronics systems together with sensors and actuators are also described. Finally, we conclude with representative systems that could exploit therapeutic and diagnostic capabilities in both surgery and wearable use cases.

S. Choi, H. Lee, Prof. T. Hyeon, Prof. D.-H. Kim
Center for Nanoparticle Research
Institute for Basic Science (IBS)
Seoul 151–742, Republic of Korea

S. Choi, H. Lee, Prof. T. Hyeon, Prof. D.-H. Kim
School of Chemical and Biological Engineering
Seoul National University
Seoul 151–742, Republic of Korea
E-mail: dkim98@snu.ac.kr

Dr. R. Ghaffari
MC10 Inc., 9 Camp St., Cambridge, MA 02140, USA

Dr. R. Ghaffari
Research Laboratory of Electronics
Massachusetts Institute of Technology
77 Massachusetts Ave., Cambridge, MA 02139, USA

2. Bio-integrated Flexible and Stretchable Systems

Figure 1 shows examples of bio-integrated electronics/optoelectronics using flexible and stretchable devices. Electrophysiological signals from the brain (e.g., EEG, electrocorticography (ECoG)) consist of complex neural activity patterns, which provide insight into normal brain function as well as neurological disorders, including epilepsy, dementia, Parkinson's disease, and restless leg syndrome (left top). Similarly, electrophysiological signals from the heart are coordinated by similar electrical signals, which provide critical insight into normal cardiac function as well as dysfunctions such as arrhythmias (center bottom). These biological signals emanate from soft and distributed cells and tissues, which are orders of magnitude smaller than the medical systems being applied to probe them. Novel microscale and nanoscale sensor designs, in arrayed formats, are thus required for measuring these fine signals. Sensor material properties, geometry (i.e., surface area), and conformal interfacial contact govern the sensing properties of these systems (e.g., signal to noise ratio). Furthermore, the mechanical properties of individual sensors must be closely matched with those of target organ tissues.

Additional circuits, sensors (e.g., strain gauges, thermal flux sensors), and actuators (LEDs, pacing/ablation electrodes) have been designed with these design considerations in order to enable conformal integration with soft and curvilinear organs. A few noteworthy examples include vision prosthesis systems consisting of stretchable photodiode arrays for image detection[28] and injectable flexible LED arrays for optogenetic applications[30] (left top). Minimally invasive systems have also exploited the soft, stretchable mechanical properties of bio-integrated electronics/opto-electronics. Instrumented balloon catheters integrated with stretchable electrodes and sensors have recently been demonstrated[31] to provide sensing and feedback therapy during cardiac mapping and ablation[32] procedures. Endovascular stents instrumented with flexible sensors and microelectronics for monitoring blood hemodynamics and the physical properties of arteries have also been recently shown to provide sensing capability onboard an otherwise purely mechanical system.[33]

Wearable bio-integrated systems consist of a similar class of flexible/stretchable sensors and electronics as in minimally invasive and implantable applications; however, these skin-based sensors and electronics have a different set of electrical, mechanical, and optical constraints during monitoring, storing, analyzing, and transferring of data from the surface of human skin (right top).[34] Artificial skin instrumented with sensors and actuators, constitutes another important branch of skin electronics for advanced prosthetics applications (left middle).[29] Transdermal drug delivery using nanoparticles loaded with pharmacological agents and activated with heat or electric field has been demonstrated in combination with these skin-based monitoring capabilities (right bottom),[34,35] thereby achieving both therapy and diagnostic capabilities onboard the same system. In the following sections, we review recent advances in these flexible and stretchable bioelectronic systems at the materials, device designs, and systems level. we present key demonstrations in implantable, minimally invasive, and wearable healthcare that highlight their important clinical needs.

Suji Choi received her B.S. (2012) from the School of Chemical Engineering at Sungkyunkwan University. Under the supervision of Prof. Dae-Hyeong Kim, she is working on the fabrication and application of stretchable nanocomposite.

Hyunjae Lee received his B.S. (2010) from the School of Chemical and Biological Engineering at Seoul National University. Under the supervision of Prof. Dae-Hyeong Kim, he is working on the fabrication and application of stretchable electrochemical sensors.

Dae-Hyeong Kim received his B.S. (2000) and M.S. (2002) degrees from the School of Chemical Engineering at Seoul National University. He obtained his Ph.D. (2009) from the department of Materials Science and Engineering at the University of Illinois at Urbana-Champaign. Since he joined the faculty of the School of Chemical and Biological Engineering at Seoul National University in 2011, he has focused on stretchable electronics for bio-medical and energy applications.

3. Nanomaterials, Assembly, and Device Designs for Flexible and Stretchable Electronics

Figure 2a shows representative forms of nanomaterials (0D, 1D, and 2D) for flexible and stretchable devices. The nanoscale dimensions of the materials dramatically decrease flexural rigidity of devices while acting as electrodes, transport channels, and light-emitting/photon-absorption materials. Zero dimensional nanoparticles (NPs; left top) have unique properties due to quantum confinement and large surface area.[36,37] One dimensional carrier transport is more efficient in nanowires (NWs; right top)[38] and carbon nanotubes (CNTs; left bottom)[39] compared to transport properties in NPs. The aligned configurations and/or percolated networks form electronic devices with robust interconnections in channels and
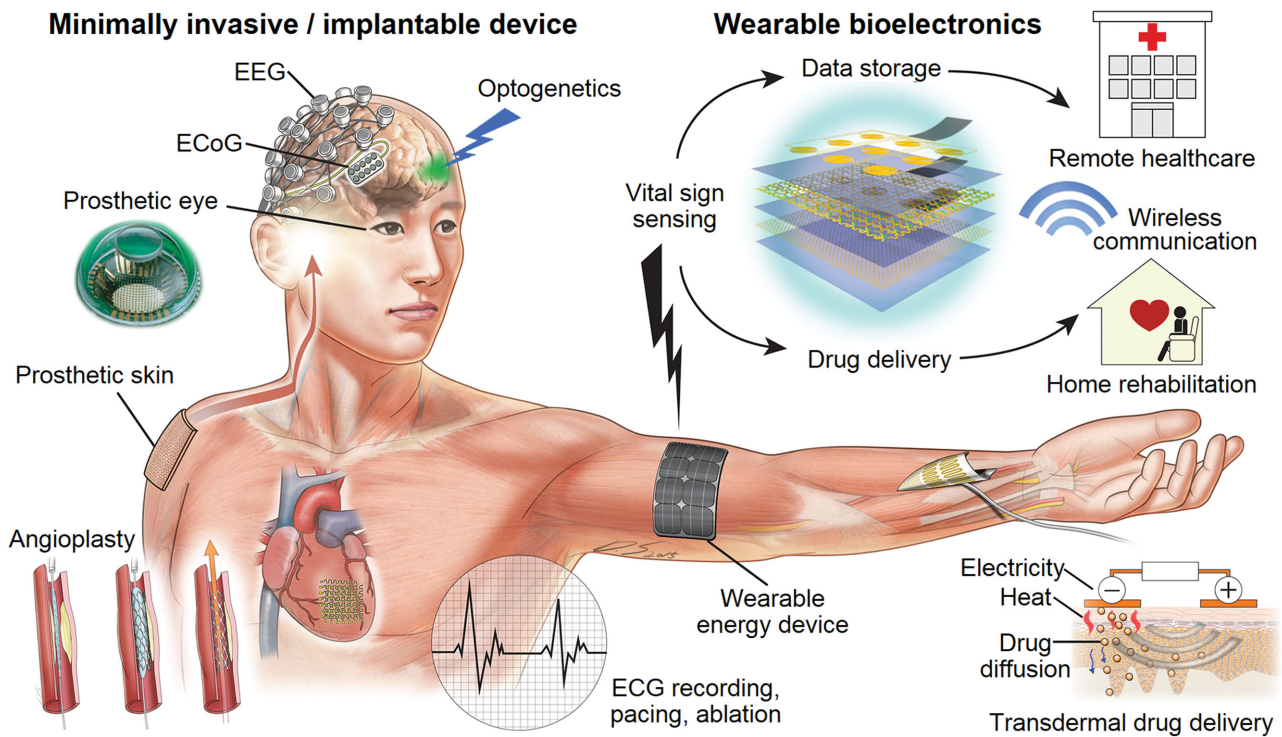
Figure 1. Bio-integrated flexible and stretchable systems. Schematic illustration of bio-integrated electronics in development today across a broad range of biomedical applications. Minimally invasive and implantable devices include electrophysiological sensors (ECoG, ECG), angioplasty tools, prosthetic eye/skin, and optoelectronic nerve stimulator, etc. Wearable bioelectronics include physiological sensors (pressure, strain, temperature sensors) integrated with transdermal drug delivery devices and data storage devices. Continuous monitoring and real time feedback therapy are performed in conjunction with the wireless communication. Energy supply module is an essential component to bioelectronics systems for mobile and personalized healthcare. Reproduced with permission.[28,29] Copyright 2008, Copyright 2014, Nature Publishing Group.
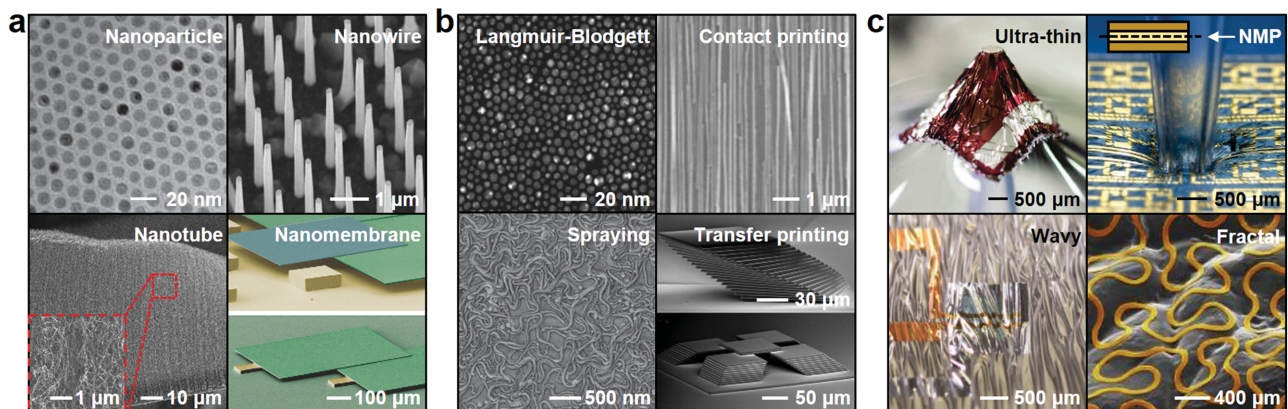

Figure 2. Nanomaterials, assembly, and device designs for flexible and stretchable electronics. a) Representative forms of nanomaterials: iron oxide nanoparticles (0D; left top), GaAs vertical NWs (1D; right top), vertical aligned carbon nanotube (CNT) (1D; left bottom), and Si NM (2D; right bottom). Reproduced with permission.[36,38–40] Copyright 2004, Nature Publishing Group, Copyright 2014, American Chemical Society, Copyright 2014, Wiley-VCH, Copyright 2012, Wiley-VCH, respectively. b) Representative assembly method for nanomaterials. Langmuir-Blodgett assembly of nanoparticles (left top), contact printing of vertical growth Si NWs (right top), spraying coating of CNT (left bottom), and Si NMs stacked by transfer printing (right bottom). Reproduced with permission.[16,41–43] Copyright 2003, American Chemical Society, Copyright 2008, American Chemical Society, Copyright 2011, Nature Publishing Group, Copyright 2010, National Academy of Sciences USA, respectively. c) Device design strategies for flexible/stretchable electronics. Ultrathin (left top), neutral mechanical plane (NMP) (right top), wavy (left bottom), and fractal (right bottom) structures enhance the system-level deformability. Reproduced with permission.[1,44–46] Copyright 2012, Nature Publishing Group, Copyright 2008, AAAS, Copyright 2013, Nature Publishing Group, Copyright 2014, Nature Publishing Group, respectively.

electrodes. Two dimensional NMs (right bottom)[40] show enhanced charge transport characteristics in planar device structures. The decreased rigidity owing to nanoscale dimensions helps mitigate the risks of mechanical failures under flexing/stretching cycles.

In the large area array of micro-/nanodevices, the uniformity of device performance is a key requirement. When nanoscale materials are uniformly fabricated/synthesized and assembled/integrated with the thickness range of less than a few micrometers, the ultrathin architecture of assembled layers decreases flexural rigidity[47] and minimizes induced strain.[22] Figure 2b shows examples for the assembly of 0D, 1D, and 2D materials. Langmuir-Blodgett (LB) technique utilizes an air-water interface to assemble a uniform, large area monolayer of nanomaterials (left top).[41] Repeating the LB process can form double or triple monolayers. The dry contact printing is another effective method to align vertically grown NWs (right top).[42] Contacting and sliding transfer NWs onto the receiver substrate. Dispersed 1D nanomaterials in a solution, such as CNTs, can be spray-coated (left bottom),[16] creating a uniform random network of CNTs over large areas. 2D NMs are transfer printed using elastomeric stamps (right bottom).[43]

In addition to the intrinsic flexibility of nanomaterials, advanced device design strategies have been used to enhance system-level deformations, as shown in Figure 2c. The induced strains are linearly and inversely proportional to thickness and bending radii, respectively. Reducing device thickness, therefore, decreases induced strains at the same bending radius (left top).[44] Locating active regions between top and bottom layers of the same structures, i.e., in the neutral mechanical plane (NMP) region where compressive and tensile strains are compensated, mitigates risks of mechanical fractures (right top).[45] Buckling enables not only bending but also stretching through elongation and contraction of wavy structures (left bottom).[1,48] Large scale stretchability is obtained via fractal/serpentine structures (right bottom).[46] These novel device structures enable new classes of wearable/implantable systems.

4. Flexible and Stretchable Bioelectronics Systems Using Established Materials

Soft bio-integrated electronic/optoelectronic systems require high quality materials, novel processes, and unconventional design strategies to achieve high performance as well as flexibility and stretchability. In this section, we introduce several different classes of sensors, associated circuits, and power modules in ultrathin, deformable formats to achieve differentiated mechanical properties from existing conventional electronics. These systems are applied in non-invasive, minimally-invasive and implantable applications where diagnostic monitoring and therapeutic actuation are required.

4.1. Epidermal Electronics

Strain and/or pressure sensors are widely employed in skin-based devices to detect motions (e.g., activity, tremor), cardiac signals (e.g., heartbeat, pulse shape), blood pressures, respiration conditions, and mechanical properties of skin. **Figure 3**a
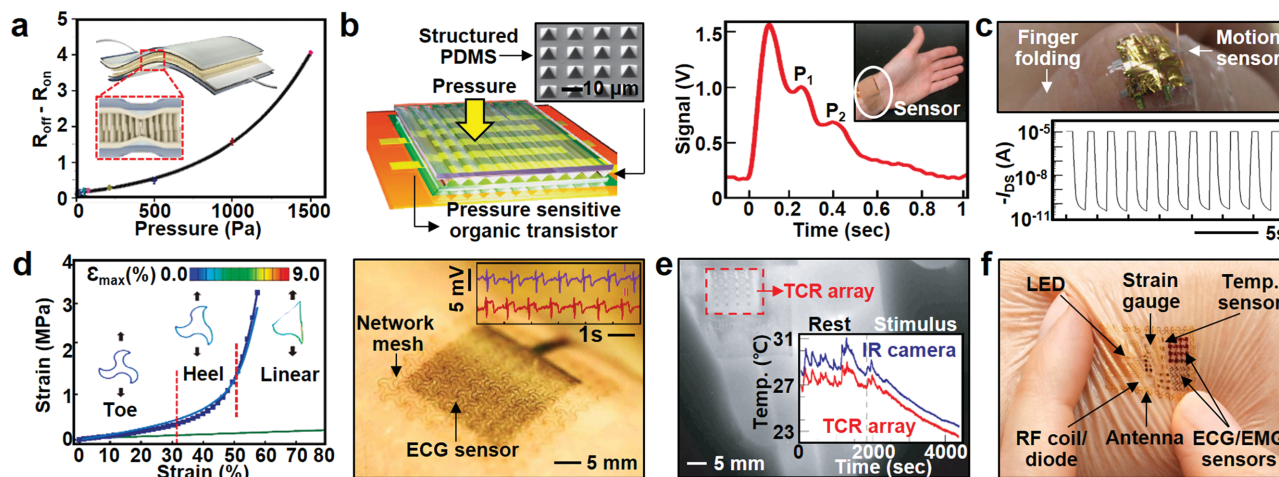

Figure 3. Epidermal electronics. a) Multiplexed, flexible strain-gauge array using an interlocked structure of Pt-coated polymer fibers. The difference of the electrical resistance between on and off contact ($R_{off} - R_{on}$) is measured as a function of applied pressures. Reproduced with permission.[49] Copyright 2012, Nature Publishing Group. b) Flexible polymer transistor sensors using micro-structured PDMS as a gate dielectric layer (left). The highly sensitive pressure sensor attached on the wrist monitors pulse waves from the radial artery (right). Reproduced with permission.[13] Copyright 2013, Nature Publishing Group. c) Stretchable motion sensor based on the organic transistor array detects finger motions (bottom). The device is attached by the PVA adhesive gel (top). Reproduced with permission.[52] Copyright 2014, Nature Publishing Group. d) The stress-strain response of the soft composite with a triangular lattice geometry: experimental (blue line) and computational (line with squares) data (left). Optical image of a skin-laminated ECG sensor on the forearm. The inset shows ECG signals measured by using the devices (right). Reproduced with permission.[53] Copyright 2015, Nature Publishing Group. e) IR camera image and corresponding temperature sensor measurement data (inset) of a palm under resting state and after stimulus. Reproduced with permission.[14] Copyright 2013, Nature Publishing Group. f) An integrated epidermal electronic system with multiple sensors (strain, temperature, ECG, EMG sensor) and other functional units (LED, RF coil/diode, antenna). Reproduced with permission.[3] Copyright 2011, AAAS.

shows flexible strain gauges composed of vertical polymer rod structures coated with platinum.[49] Resistance changes in the interlocked conducting arrays allow detection of changes in pressure, shear force, and torsion. The high sensitivity of the hair-like sensor arrays allows capture of faint signals, like pulse from the wrist.[50] Figure 3b highlights another unique engineering approach for sensing pressure perturbations on human skin.[13] The micro-structured, soft gate dielectric of an organic transistor (left) has a measurable channel conductance, which can be modulated with an applied external pressure,[51] such as pulse wave signals measured from radial artery (right).

Further improvements in the signal to noise ratio can be achieved by reducing the bending stiffness and thickness of the system, or alternatively, by enhancing adhesion of the device to the skin. Ultrathin devices below tens of micrometers in thickness with gel-type adhesives, for example, have high sensitivity (Figure 3c).[52] Another strategy to achieve reduced stiffness is to adopt serpentine pattern designs. Mechanically optimized serpentine geometries, such as the optimized arc angle in the 2D serpentine filament,[46] can help soft network composites to match with the mechanical property of human epidermis (Figure 3d left).[53] These design improvements provide better conformal contact, which gives rise to reduced effective impedance and noise for ECG measurements (right). Strategies that minimize stiffness are also applied for devices that spatially map (Figure 3e), hydration[14] and the elastic mechanical properties of skin.[54]

A representative example combines these multiple sensing modalities and device design strategies to yield a functional epidermal electronics system (Figure 3f).[3] Other functional units integrated in the system include a display component (LED) and wireless communication units (RF coil and high frequency diode). Although these skin-based devices are successfully applied for physiological and electrophysiological sensing, thermal mapping, and wound healing measurement,[55] high capacity ultrathin batteries, wireless communication[11] via radio frequency connectivity, and other optoelectronic functionality are required to achieve practical utility in clinical applications. The multifunctional epidermal electronic system can be fabricated over large area by simply cutting and transferring electronic devices onto target substrates.[56]

4.2. Invasive Applications

Similar to the methodology employed for epidermal electronics, invasive medical systems consisting of ultrathin, stretchable circuits exploit similar mechanical properties in order to laminate or interface on the surface of organs. **Figure 4**a shows a balloon catheter integrated with ECG/tactile/temperature/flow sensors and RF ablation electrodes.[31] The stretchable designs are well suited for repetitive inflation/deflation cycles of the balloons, which can accommodate large strains exceeding ≈130%. A multifunctional system, in the format of a sleeve, contains a similar class of multifunctional devices, such as sensors for spatiotemporal epicardial monitoring (e.g. ECG, pH) (Figure 4b)[57] and actuators for defibrillation and ablation.[58] The soft, elastic encapsulating membrane provides robust, conformal contact with the epicardium under minimal mechanical loading stresses applied to the heart.

Incorporating high performance Si multiplexing circuits enables significant new capabilities in high spatiotemporal resolution mapping (Figure 4c).[59] High density, multiplexed electrode arrays consisting of active circuitry have been
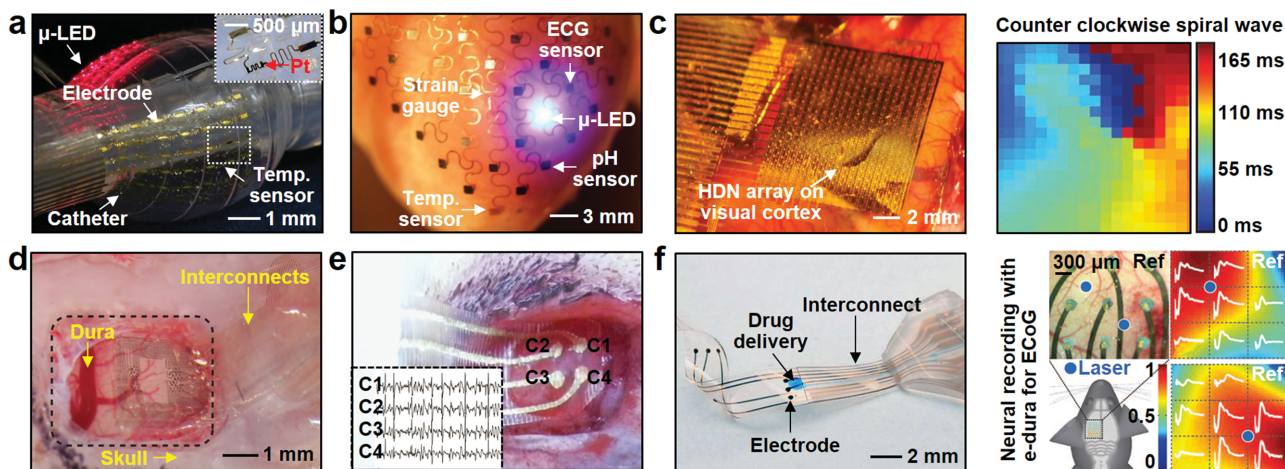

Figure 4. Invasive applications. a) Multifunctional balloon catheter in an inflated state, equipped with temperature sensors, microscale light-emitting diodes, and tactile sensors (facing downward). The inset image shows a Pt-based temperature sensor. Reproduced with permission.[31] Copyright 2011, Nature Publishing Group. b) An optical camera image of 3D multifunctional integumentary membrane (3D-MIM) with ECG electrodes, strain gauge, LED, pH sensor, and temperature sensor, enveloping a rabbit heart ex vivo. Reproduced with permission.[57] Copyright 2014, Nature Publishing Group. c) An optical camera image of a flexible, high-density active electrode array placed on the visual cortex of cat to map neural activities (left). Two-dimensional mapping data of a cat's brain (right). Reproduced with permission.[59] Copyright 2011, Nature Publishing Group. d) PEDOT:PSS-based electrodes that cover the cortical surface of a rat. Reproduced with permission.[60] Copyright 2015, Nature Publishing Group. e) An optical camera image of highly stretchable gold nanobelt electrodes on a rat brain (left). ECoG signals recorded from an epileptic rat (inset). Reproduced with permission.[61] Copyright 2015, Wiley-VCH. f) An optical camera image of a soft, biocompatible electronic dura (e-dura) (left). The spatial mapping data from the e-dura during laser stimulation on the brain (right). Reproduced with permission.[62] Copyright 2015, AAAS.

demonstrated to conformally contact the surface of the cortex (left) and record sleep spindles, visual evoked responses, and micro/macro seizures (right) in live animal models. The signal quality of electrophysiological recording was further enhanced with conductive polymers, such as poly(3,4-ethylenedioxythiophene) doped with poly(styrene sulfonate) (PEDOT:PSS) as shown in Figure 4d.[60] Conductive polymers that interface with cortical neurons decrease electrochemical impedance and enable high quality recordings of local field potentials and action potentials.[63,64] Adding stretchability to sensors further enhances conformal contact, giving rise to better signal outputs. For example, the combination of an elastomeric substrate with gold nanobelts provides 130% stretchability and robust recording of ECoG from live epileptic rats (Figure 4e).[61] Integration of soft microfluidic delivery mechanisms and stimulation electrodes in an e-dura mater (Figure 4f left)[62] enables electrochemical and electrical stimulation on spinal cord, as a way to restore motion in paralyzed rats. The soft electrode array of the e-dura also records neural signals over cortical surfaces (right).

4.3. Stretchable Optoelectronic Devices

Although optoelectronic device research, including photodetector, phototransistor, and LED technologies are widely implemented in biomedical applications (e.g. light-based mechanical sensors,[65] visual prosthesis,[66] and optogenetics,[67] conventional optoelectronic devices have limitations due to the mechanical mismatch between soft, curvilinear human body

and rigid optoelectronic devices. Soft, stretchable optoelectronics for stimulation and sensing provide new possibilities for phototherapy and optogenetics research, while solving these issues. **Figure 5**a left, for example, shows images of stretchable LED arrays, undergoing twisting (360° and 720°).[68] The stretchable micro-LED array can be mounted on various substrates including elastomeric ones for various medical-related functionalities. As a representative example, micro-LED arrays on an inflatable balloon catheter easily gain access to the target sites inside the human body, such as endovascular and endocardial surfaces, and enable light-based sensing and therapies in vivo. Moreover, light-based stimulation of skin wounds using micro-LED arrays mounted on sutures can help accelerate healing processes (right). The close proximity between the LEDs and target tissue maximizes photon absorption over a given surface area. Photodetector arrays are in a similar ultrathin and stretchable format and are now being applied for ocular prosthesis. A hemispherical photodetector array inspired by the arthropod's eye is shown in Figure 5b left.[69] The microlens and hemispherical design provide wide field of view and minimize image distortions, respectively (right).

4.4. Stretchable Power Supply Devices

Stretchable energy harvesting and energy storage devices that can be intimately integrated with soft bioelectronics are required to continuously power supply to portable and mobile health monitoring systems. **Figure 6**a (left) shows stretchable, wavy organic solar cells in stretched and
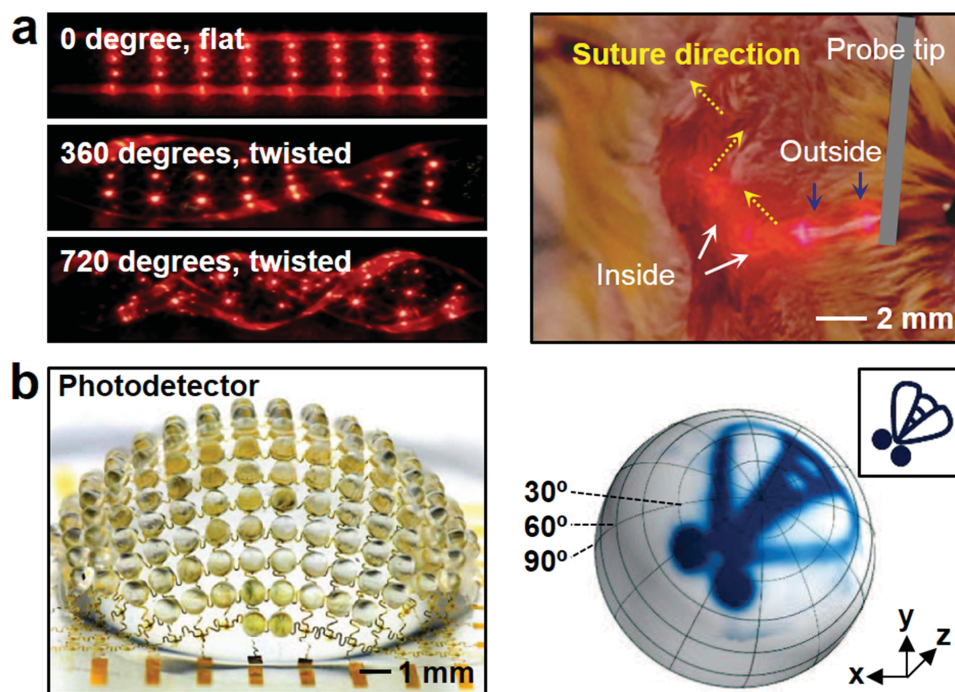

Figure 5. Stretchable optoelectronic devices. a) An optical camera images of a μ-ILED array in a flat (0°) and twisted (360° and 720°) state (left). An in vivo animal experiment demonstration of the light-emitting suture (right). Reproduced with permission.[68] Copyright 2010, Nature Publishing Group. b) An optical camera image of a photodetector array inspired by an arthropod eye (left). An illustration of a fly is captured by the photodetectors and rendered on a hemispherical surface (right). Reproduced with permission.[69] Copyright 2013, Nature Publishing Group.
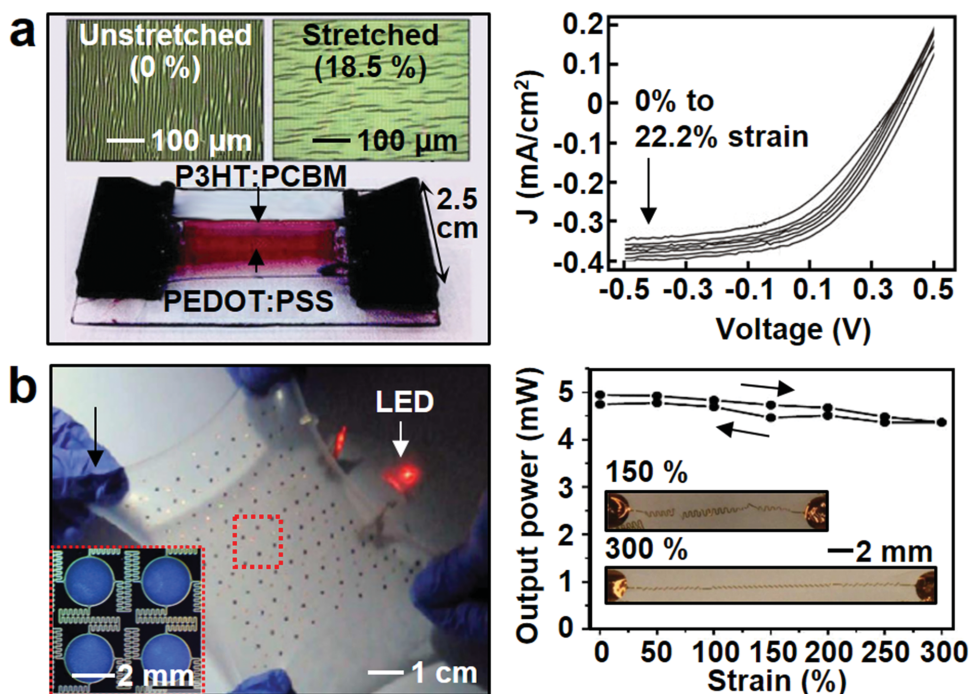
Figure 6. Stretchable power supply devices. a) A photograph of a stretchable solar cell (left) and its optical microscope images before and after 18.5% stretching (inset). Photovoltaic device characterization (I–V curve) under applied tensile strain from 0% to 22.2% (right). Reproduced with permission.[70] Copyright 2011, Wiley-VCH. b) An optical camera image of a stretchable battery under biaxial stretching (≈300%) without noticeable dimming of a red LED. The inset shows its magnified view (left). Output power data of a stretchable battery at various applied strains. The inset shows its serpentine interconnection under applied tensile strain (right). Reproduced with permission.[71] Copyright 2013, Nature Publishing Group.

unstretched configurations with active (P3HT:PCBM) and anode (PEDOT:PSS) regions.[70] This device exhibits stable performance in response to applied strains reaching ≈22.2% (right). In addition to energy harvesting components, stretchable energy storage devices (e.g., battery, supercapacitor) are needed. Stretchable rechargeable batteries coupled together with serpentine interconnect design and low modulus silicone elastomers can be stretched up to ≈300% without noticeable dimming of the connected LED (Figure 6b left),[71] preserving their output powers (right). Wireless power transmission successfully recharges the stretchable battery on human skin via inductive coupling.[72–74] These stretchable energy devices and wireless power transmission/communication units provide portability/wearability for stretchable biointegrated electronics systems.

5. Flexible and Stretchable Bioelectronics Integrated with Synthesized Nanomaterials

Nanomaterials processed from established materials such as single crystal Si have been shown to have high quality electrical performance and good uniformity. In addition to these established materials, synthesized nanomaterials, processed using colloidal methods and/or chemical vapor deposition strategies, have also been shown to have unique physical, chemical, mechanical, and optical properties, extending beyond what many established materials have. The characteristics of synthesized nanomaterials are tuned depending on specific

functions and conditions required for a set of applications. Heterogeneous integration of synthesized nanomaterials with established classes of Si based nanomaterials is also feasible, and creates new opportunities for emerging soft, stretchable bioelectronics. In this chapter, we present recent advances in flexible and stretchable bioelectronics that incorporate both established and synthesized nanomaterials.

5.1. Skin-laminated Piezoresistive/Piezoelectric Sensors

Synthesized nanomaterials and their hybrids processed with established nanomaterials have enabled a variety of new sensors, including pressure, strain, and temperature sensing arrays. Exploiting the conductivity and/or piezoelectric properties of these nanomaterials in soft sensors in combination with unique mechanical and optical properties (i.e. stretchability and transparency) enables new biomedical applications. Carbon black, for example, has been widely utilized as a nanofiller for the conductive nanocomposite rubber (**Figure 7**a).[75] Patterned carbon black, in conjunction with the intrinsic softness of rubber materials, has led to novel piezoresistive strain sensor arrays in wearable formats for tracking motions and skin mechanical properties (left). The patterned conductive rubber intimately couples with skin at any location on the body, including joints, such as wrist and knee, for accurate monitoring of biomechanics (right). There are practical challenges in establishing contacts between functional 0D materials (e.g., carbon black), however, which may result in
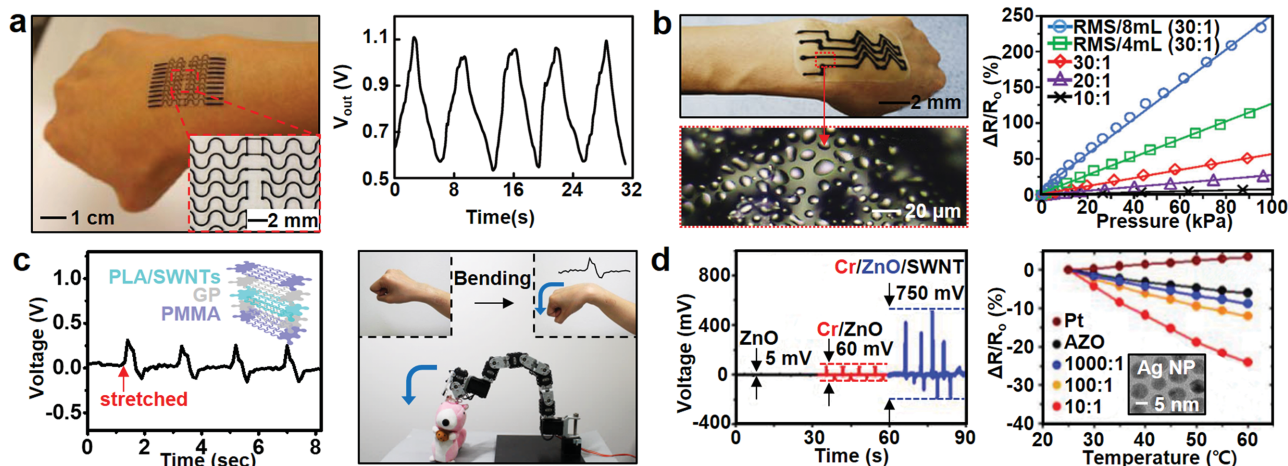
Figure 7. Skin-laminated piezoresistive/piezoelectric sensors. a) A photograph of a strain sensor array laminated on the human wrist to detect wrist motions (left). A graph of the output voltage under repeated wrist motions (right). Reproduced with permission.[75] Copyright 2012, Wiley-VCH. b) A photograph of piezoresistive strain sensor fabricated with the printed CNT-PDMS nanocomposite (left top). A magnified view shows its porous structure (left bottom). The percent resistance change of the deformed CNT-PDMS nanocomposite with (blue, green) or without (red, purple, black) porous structure as a function of applied pressures (right). Reproduced with permission.[78] Copyright 2014, Wiley-VCH. c) Piezoelectric strain sensor fabricated with a PLA/SWNT nanocomposite and its representative voltage responses under applied strains (left). An optical camera image of controlling the robot arm by using the piezoelectric strain sensor (right). Reproduced with permission.[79] Copyright 2015, Wiley-VCH. d) The output voltage of the piezoelectric strain sensor fabricated with ZnO (black), Cr/ZnO (red), and Cr/ZnO/SWNT (blue) layers (left). Percent resistance changes of temperature sensors with different Ag NP concentrations at different temperatures (right). Reproduced with permission.[15] Copyright 2015, Wiley-VCH.

reduced conductivity and higher power consumption. Percolations between 1D nanomaterials (e.g., CNTs, NWs) are much more probable due to their high aspect ratio, leading to much higher conductivity even under stretched states.[23,76,77] Figure 7b shows a porous pressure sensitive rubber-based structure composed of this kind of 1D CNT networks (left bottom),[78] which can be integrated as a pressure/strain sensor array (left top). The porous structure (made by using reverse micelle solutions) enhances sensitivity of the pressure/strain sensors further, while the percolated structure allows for large dynamic range (right).

Although piezoresistive sensors based on conductive rubbers show reliable and linear responses to external stresses, their slow signal response times impose high hysteresis effects. There have been breakthroughs of the piezoresistive sensors,[80,81] in the fast response time with a minimal dependence on temperature via tunneling resistance between 3-dimensional interlocked microdome arrays of piezoresistive composites. Meanwhile, separating responses of temperature and strain/pressure sensors represents another hurdle. As a result, many piezoelectric materials have been proposed as alternatives to piezoresistive conductive rubbers. When external forces are applied to piezoelectric materials, induced strains align dipoles and generate electric fields, which in turn, drive current flow to external circuits,[82,83] thus, the mechanical sensors based on the piezoelectric materials show self-powered operation and faster response time. Piezoelectric polymers (polylactic acid; PLA)/SWNT composites patterned and sandwiched between transparent graphene electrodes (Figure 7c) increase local induced strains and maximize signal-to-noise ratio (left).[79] This new class of piezoelectric hybrids has unique transparent optical properties and has been demonstrated for human-machine-interface applications with a natural skin look (right).

Additional material classes, including oxide NMs, semiconductor NWs, and insulators, have also been used for piezoelectric mechanical sensors. Oxide NMs have been designed as strain and a temperature sensor in skin-like formats (Figure 7d).[15] In comparison to solution-processed piezoelectric polymers, these oxide NMs are significantly more uniform and compatible with conventional mass-production manufacturing practices prevalent in the display industry. The piezoelectric properties of ZnO NMs are further enhanced by insertion of Cr (by increasing crystallinity) and SWNTs (by capturing free electrons) at the bottom and top of the ZnO layers (left). Temperature monitoring on skin is also enabled by conductive oxide NMs, such as 1 wt% Al-doped ZnO (AZO). Integration of silver nanoparticles maximizes the thermal response properties of AZO NMs, extending the sensitivity higher than conventional platinum-based temperature sensors (right). These nanomaterials have been applied for epidermal systems to monitor dynamic changes of strain and temperature on human skin.

5.2. Artificial Skins

While soft bioelectronics laminated on human skin have been established for monitoring of physiological and electrophysiological signals, soft/stretchable bioelectronics are also useful for artificial skins. A variety of sensors (e.g., mechanical and temperature sensors) integrated on plastic and/or elastomeric substrates can capture signals, simulating mechano- and thermo-receptor properties of skin tissues. **Figure 8**a shows an artificial skin composed of an integrated array of strain, pressure, temperature, and humidity sensors.[29] Si NM diodes integrated with the sensor array on elastomers (inset) enable multiplexing of each sensor for thermal and strain mapping
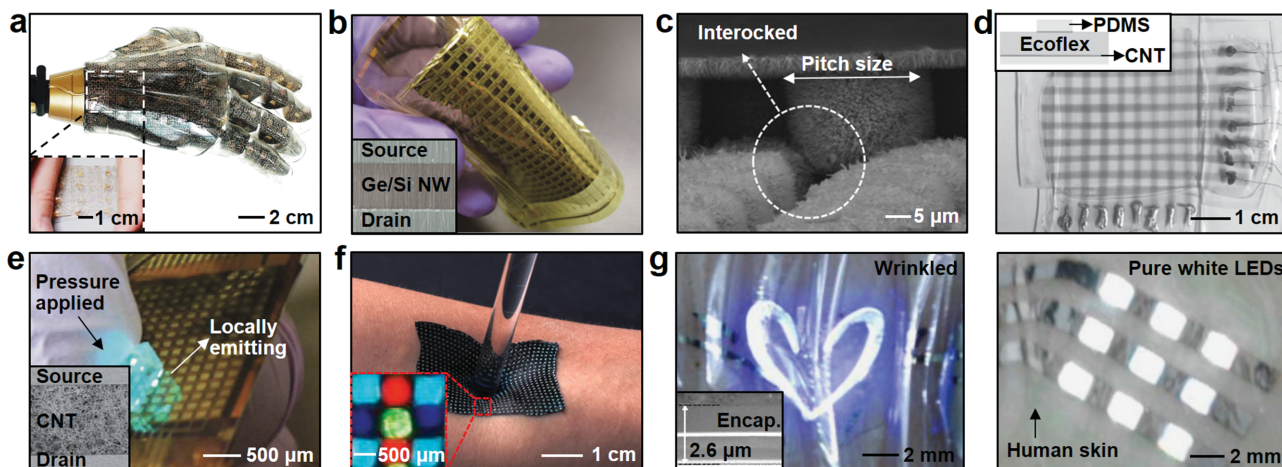
Figure 8. Artificial skins. a) An optical camera image of an artificial skin composed of stretchable sensors and actuators. The inset shows a stretched image (≈20%) of the artificial skin. Reproduced with permission.[29] Copyright 2014, Nature Publishing Group. b) A photograph of a flexible pressure sensor array using a Ge/Si NW TFT active matrix. Reproduced with permission.[84] Copyright 2010, Nature Publishing Group. c) A pressure sensor for the e-skin, which is based on the interlocking geometry of ZnO NWs. Reproduced with permission.[80] Copyright 2015, Wiley-VCH. d) A photograph of transparent, capacitive pressure sensors using a PDMS dielectric layer and CNT electrodes. Reproduced with permission.[16] Copyright 2011, Nature Publishing Group. e) An optical camera image of the interactive artificial skin. Reproduced with permission.[86] Copyright 2013, Nature Publishing Group. f) A photograph of a thermal imaging device laminated on the deformed skin. Inset shows a magnified view of the device. Reproduced with permission.[87] Copyright 2014, Nature Publishing Group. g) An optical camera image of ultrathin blue QLEDs laminated on the human skin (left). The inset shows a cross-sectional SEM image of a QLED. A photograph of a wearable white QLED array laminated on the human skin (right). Reproduced with permission.[88] Copyright 2015, Nature Publishing Group.

with high spatial and temporal resolution. Utilizing active matrix circuits based on Ge and/or Si NW TFT arrays provides enhanced spatial and temporal resolutions in pressure sensing, with minimum signal crosstalks (Figure 8b).[84] The high carrier mobility and mechanical flexibility of inorganic single crystal semiconducting NWs[85] enable these multiplexed pressure sensing arrays with low power consumption and adequate mechanical stability.

Another advantage of NW-based sensors for the artificial skin is in their extremely high sensitivity. Figure 8c shows a scanning electron microscope (SEM) image of a ZnO NW pressure sensor.[80] The interlocked structure of ZnO NWs, in particular, maximizes sensitivity and response time for static pressure detection, successfully monitoring subtle dynamic tactile stimuli. 1D carbon nanomaterials can be used as an alternative to NWs. The sensitivity of carbon nanomaterials to external stresses is greater than the conventional pressure sensitive rubbers. Furthermore, the soft nature of carbon allows for extreme bending and stretching mechanics. Figure 8d shows an example of stretchable and transparent SWNT-based mechanical sensors.[16] Its capacitive structure in an array layout enhances sensitivity, while multiplexing with low crosstalk. A unique spray process for SWNTs onto elastomeric substrates allows for uniform integration of sensor arrays over large surface areas.

Many multiplexed sensors that use nanomaterials in combination with elastomeric substrates are transparent or semi-transparent. These optical properties are well suited for epidermal optoelectronics applications, as they enable new classes of interactive artificial skin.[89] Heterogeneous integration of OLED and active matrix pressure sensor arrays in electronic skin-based systems, for example, provides instant visual responses about the location and magnitude of applied pressures (Figure 8e).[86] CNT is used as a channel material for OLED driving circuits to obtain high drive current as well as mechanical reliability (inset). For visualizing additional information about skin, such as thermal changes, thermochromic liquid crystals (TLCs) have also been used (Figure 8f).[87] However, TLCs exhibit low spatial and color resolution. Meanwhile, red/green/blue quantum dot (QD) light-emitting diode arrays have been highlighted as a next-generation display.[90] Inorganic quantum dots demonstrate better stability to environmental factors than organic light emitting materials and allow much thinner encapsulation layers.[91] Recently wearable QLEDs using a high-resolution intaglio transfer printing technique (up to 2,460 pixel per inch) were reported (Figure 8g).[88] The ultrathin structure (≈2.6 µm) of QLEDs laminated on skin shows high optoelectronic performances and stable light emitting characteristics under physical deformations (left). Pure white QLEDs are also achieved on human skin (right) by combining transfer-printed red-green-blue subpixels, which could play an important role in displaying input/output information onboard wearable systems.

5.3. Implantable Bioelectronics

Flexible and stretchable bioelectronic devices consisting of unusual nanomaterials are applicable for invasive systems used to monitor internal organs. The signals captured from implantable bioelectronic devices are processed and trigger feedback commands to co-integrated therapeutic devices. Various unique properties of nanomaterials enable clinically relevant but previously unrealized functional modes, such as high quality electrophysiological mapping and controlled drug
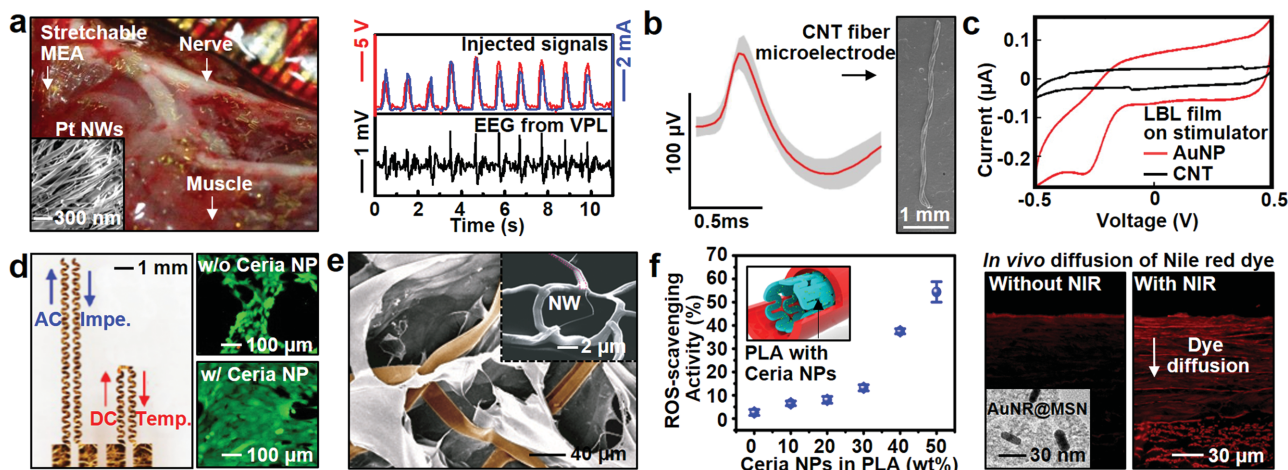
Figure 9. Implantable bioelectronics. a) An optical camera image of the stretchable MEA on peripheral nerves of a rat model (left). Electrodes decorated with Pt NWs are conformally contacted to nerves (inset). Injected electrical stimulation signals (red) deliver the current (blue) through the peripheral nerves. Corresponding EEG signals are detected from the ventral posterolateral nucleus (VPL) (black). Reproduced with permission.[29] Copyright 2014, Nature Publishing Group. b) The SEM image of CNT microelectrode for recording brain signals (right) and the averaged neural waveforms recorded by the CNT microelectrode (left). Reproduced with permission.[92] Copyright 2015, American Chemical Society. c) Electrochemical characterization of a gold nanoparticle (red) and CNT (black) film assembled by the LBL method. Reproduced with permission.[93] Copyright 2012, American Chemical Society. d) Multifunctional and soft cell-culture platform (left). Cell viability can be increased in the presence of ceria nanoparticles (right). Reproduced with permission.[94] Copyright 2015, American Chemical Society. e) A SEM image of the macroporous nanoelectronic scaffold with alginate. The inset shows a magnified view of the original nanoelectronic scaffold. Reproduced with permission.[95] Copyright 2012, Nature Publishing Group. f) Bioresorbable electronic stent integrated with therapeutic nanoparticles (inset). A graph of the ROS scavenging activity of the ceria NPs as a function of NP concentrations (left). A TEM image of the gold nanorod core/mesoporous silica nanoparticle shell (inset). The drug loaded on the silica shell is diffused into endothelium by the hyperthermia effect of gold nanorod core induced by the NIR radiation (right). Reproduced with permission.[33] Copyright 2015, American Chemical Society.

delivery. The Pt NWs decorated on stretchable multi-electrode arrays (MEA), for example, are used as a neural interface to peripheral nerves (**Figure 9**a, left).[29] The low impedance and large surface area of Pt NWs on the electrodes facilitate efficient electrical stimulation to/recording from nerve fibers with response to externally detected signals (right top). This stimulation pattern is successfully observed from ventral posterolateral nucleus (VPL) in the form of synchronized sharp spikes (right bottom). In addition to Pt NWs, ceria NPs can be applied to mitigate the risks of reactive-oxygen-induced inflammations. In addition to these inorganic nanomaterials, soft conducting carbon materials such as CNT fibers may also be applied. Figure 9b shows CNT electrodes on the motor cortex of a mouse. The device detects high frequency single unit spikes with remarkably low impedance.[92] The high charge storage capacity of CNT fibers enables effective long term in vivo neural recordings. Au NPs assembled by layer-by-layer (LBL) methodologies on these types of electrodes further increases the charge storage capacity and forms high quality neural interface (Figure 9c).[93]

In addition to recording of electrophysiological signals, monitoring of impedance/conductivity is important in determining tissue viability/activity.[96] Proliferation and differentiation of transplanted cells in tissue regeneration therapies, for example, must be monitored. Figure 9d shows a multifunctional cell culture transplant device, with stretchable gold nanoribbon/graphene sensors/cell-aligners for impedance, conductance, and temperature monitoring during proliferation/differentiation of cell sheets and their transplant.[94] The high adhesion of ECM proteins to graphene promotes cell proliferation and differentiation.[97] The cell sheet is fully differentiated and transplanted to diseased sites in vivo. Meanwhile, a flexible Si NW sensor network can be integrated with various biomaterials in a macroporous form for cellular monitoring during cell culture (Figure 9e).[95] This 3D Si NW sensing scaffold provides higher sensitivity than conventional macro-devices during monitoring of cellular activities. The 3D Si NW electronic mesh can be injected into the internal cavity of the biotic system via a minimally invasive route using a syringe to monitor internal mechanical strain and electrophysiological activities.[98]

In addition to monitoring electrophysiology at neuron and muscle interfaces, there are new classes of endovascular systems that can address major vascular diseases. Bioresorbable stents integrated with sensors (e.g., blood flow and temperature sensor) can target diseased sites in blood vessels to monitor reperfusion and restenosis mechanisms (Figure 9f).[33] Co-integrated ceria NPs onboard these smart stents can scavenge reactive oxygen species (ROS) through catalytic reactions (left). Collected data from blood flow sensors during/after angioplasty are stored in nonvolatile memory onboard the stent and wirelessly transmitted using an antenna design that is integrated in the metal strut of the stent itself. Localized drug delivery is tuned by modulating stent surface temperature (right). The Au nanorod core is coated with drug-loaded mesoporous silica shell (AuNR@MSN) and integrated on the stent. Near IR laser guidance, delivered with a catheter, locally increases temperature and accelerates release of loaded drugs while the integrated temperature sensor detects the temperature profile to prevent overheating.
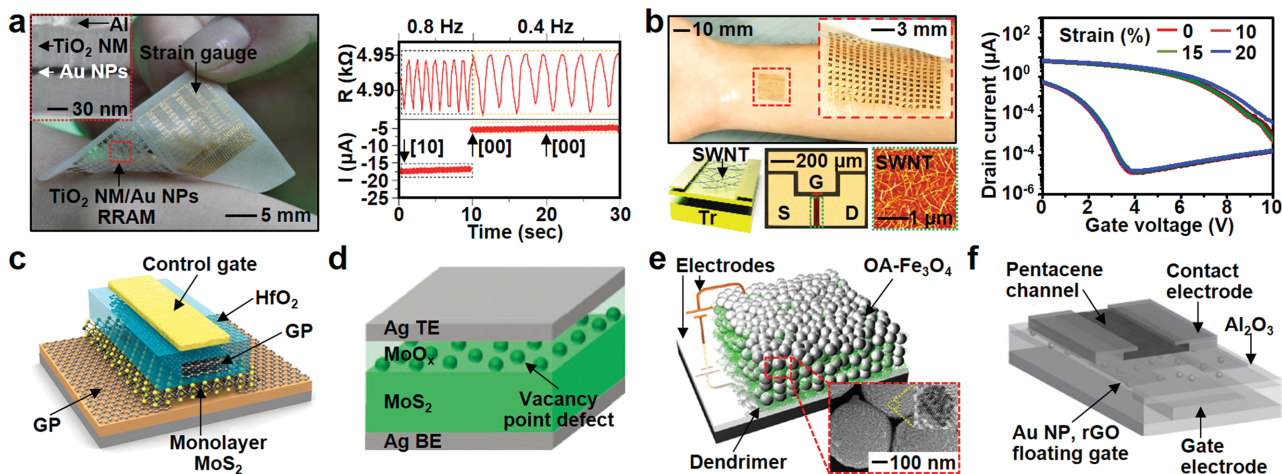
Figure 10. Data storage devices. a) An optical camera image of a wearable electronic patch (left). Detection of the simulated hand tremor and data storage in the memory cells using a multi-level-cell operation (right). Reproduced with permission.[34] Copyright 2014, Nature Publishing Group. b) An optical camera image of SWCNT-based memory devices laminated on human skin (left). Transfer characteristics of SWCNT-based charge-trap floating gate memory devices under applied strain of 0 ≈ 20% (right). Reproduced with permission.[99] Copyright 2015, American Chemical Society. c) A schematic illustration of a nonvolatile memory device based on a MoS_2/graphene heterostructure. Reproduced with permission.[100] Copyright 2013, American Chemical Society. d) A schematic illustration of a solution-processed MoO_x/MoS_2 memristor. Reproduced with permission.[101] Copyright 2015, Nature Publishing Group. e) A schematic illustration of a nonvolatile memory device based on dendrimer/Fe_3O_4 multilayers. Reproduced with permission.[102] Copyright 2013, American Chemical Society. f) A schematic illustration of a flash memory device based on a rGO-Au NP hybrid double-floating-gate. Reproduced with permission.[103] Copyright 2013, Wiley-VCH.

5.4. Data Storage Devices

Continuous monitoring of important biological signals require storage and analysis of this recorded data. Ultrathin data storage modules have been co-integrated onboard these epidermal systems. Nanomaterials have enabled these nonvolatile data storage devices to exhibit high performances and require low operation power. **Figure 10**a left shows a system level demonstration of a wearable nonvolatile memory device integrated with a Si NM-based strain gauge array.[34] The strain changes measured by wearable sensors can track tremors of Parkinson's disease patients. For low power consumption, Au NPs are assembled on TiO_2 NM between top and bottom Al electrodes via a LB assembly technique (inset). The tremor frequencies are stored in memory cells using the multi-level-cell operation (right). The stored data can then be analyzed to diagnose patient conditions.

Although inorganic NM-based memory devices have proven reliability and high performance, soft semiconducting materials have mechanical advantages particularly under repetitive deformations and accumulated fatigue cycles. On this ground, charge-trap floating gate memory based on a soft carbon nanomaterial (SWNT) has been fabricated in a wearable format (Figure 10b left).[99] The carrier charging/discharging into/from hydroxyl groups of SWNTs result in a large memory window. Carbon materials are compatible with soft deformable substrates and enable excellent mechanical reliability. The soft wearable memory arrays do not undergo mechanical fractures during physical deformations of human skin (right).

In addition to oxide NMs and SWNTs, various novel nanomaterials have been utilized to maximize the performance of nonvolatile memory modules. A monolayer MoS_2 is utilized for FET-based flash memory (Figure 10c).[100] The MoS_2 floating gate memory achieves fast charging/discharging and a large on/off ratio between programing and erase states. More recently, ultralow operation voltage of resistive memory by using MoS_2 and MoO_x is reported (Figure 10d).[101] Due to low operating voltages, this memory consumes minimal energy, which is ideal for power-constrained applications for implantable/wearable bioelectronics. For more efficient charge trap/confinement, nanoparticle films assembled by a LBL method have been applied for nonvolatile memory modules (Figure 10e).[102] Successive adsorption of NPs with hydrophobic ligands and amine-terminated dendrimers form multilayered charge traps for efficient confinement of carriers. Figure 9f shows another example of self-assembled floating gates.[103] An assembly of Au NPs and reduced graphene oxides (rGOs) is used as a double floating gate. This double floating gate improves memory performances, i.e., retention and window margins.

5.5. Thermal and Electrical Actuators for Physical Therapy and Drug Delivery

Various classes of thermal/electrical actuators have been used as therapeutic devices for several decades across a broad range of applications. These actuators deliver heat or electrical impulses and/or accelerate diffusion of drugs in a transdermal manner. Their wearable forms increase the efficiency and effectiveness of physical and/or chemical therapies. Nanomaterials enable key functions in these wearable systems. **Figure 11**a shows a soft, thin, and stretchable heater fabricated by a composite of ligand exchanged silver nanowires (Ag NWs) and elastomer (styrene-butadiene-styrene; SBS).[104] The high percolation of Ag NWs and the heater design of a serpentine shape enable stable joule heating and effective heat transfer to the
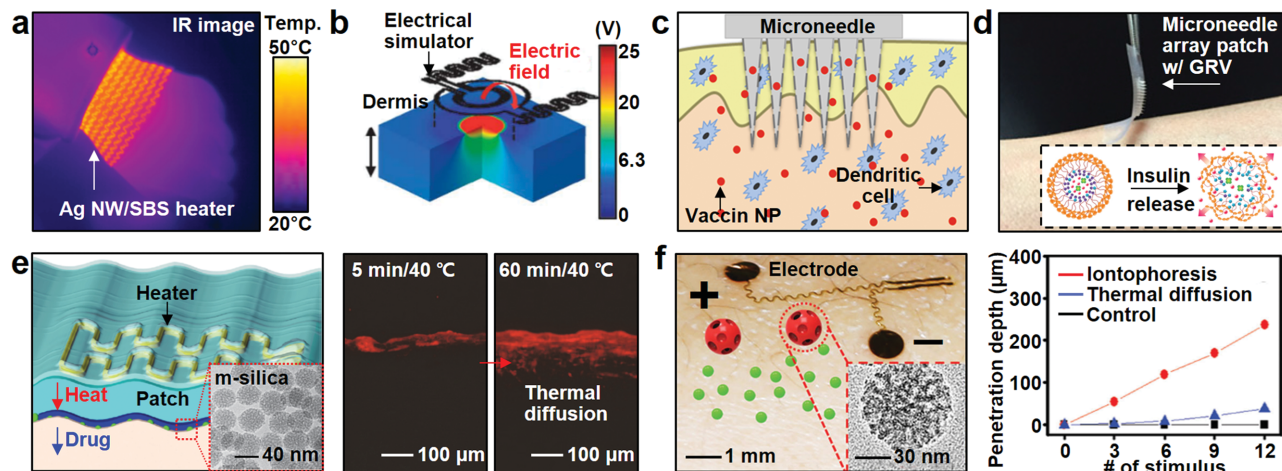
Figure 11. Thermal and electrical actuators for physical therapy and drug delivery. a) An infrared camera image of a wearable heater composed of Ag NWs/elastomer with a serpentine mesh design. Reproduced with permission.[104] Copyright 2015, American Chemical Society. b) Wearable electrical stimulator based on graphene/Ag NWs hybrid. Reproduced with permission.[79] Copyright 2015, Wiley-VCH. c) A schematic illustration of a micro-needle array containing vaccine-loaded nanoparticles. Reproduced with permission.[107] Copyright 2013, American Chemical Society. d) Glucose responsible vesicles (GRV) loaded on the micro-needle patch. Reproduced with permission.[108] Copyright 2015, National Academy of Sciences USA. e) Transdermal drug delivery using a wearable heater (left). Drug loaded in mesoporous silica nanoparticles is released by thermal stimuli. Effective drug diffusion into the pig skin, confirmed with the fluorescence imaging (right). Reproduced with permission.[34] Copyright 2014, Nature Publishing Group. f) Transdermal drug delivery using the iontophoresis (left). Penetration depth linearly increases depending on the number of the electrical stimulus (right). Reproduced with permission.[35] Copyright 2015, Wiley-VCH.

moving joints. The high conductivity of stretchable electrodes of the nanomaterial-hybrid (graphene and Ag NWs)[105,106] also enables direct electrical pulse injections into/through the skin. Conformal contact by the soft nature of electrodes facilitates the efficient electrical stimulation on the skin (Figure 11b).[79]

Skin-based therapies can be delivered using a special class of transdermal drugs, which can diffuse through skin and into the bloodstream. One widely used mode of transdermal drug delivery relies on micro-needles. Figure 11c shows a dissolvable micro-needle array containing antigens encapsulated by/in PLGA nanoparticles, which prolongs retaining time of vaccines.[107] Another representative application of this micro-needle array is the regulation and delivery of insulin with nano-sized glucose responsive vesicles (GRVs) (Figure 11d).[108] GRVs automatically are dissociated and release insulin when the hyperglycemia occurs. Although micro-needles are rapid and effective, skin infection and/or irritation due to allergic response or in sensitive skin could be accompanied. Wearable heater and electrical actuator integrated together with drug-loaded nanoparticles avoid these problems. Figure 11e left shows thermally-actuated transdermal drug delivery using a wearable heater.[34] The drug is loaded into mesoporous-silica nanoparticles. The sensor data determines the drug release rate by modulating the temperature of the patch. As the patch/skin temperature increases, the diffusion rate/depth also increases (right). Although thermal diffusion can deliver both polar and nonpolar drug, it is slow. Polar drugs can be delivered with a faster speed under the electric field built by wearable electrodes in the iontophoresis system (Figure 11f left).[35] In this case, potential concerns in the thermal diffusion of drugs, such as low temperature burns and thermal denaturation of drugs, can be prevented. The in vivo study on BALB/c-mouse skin shows

that the drug diffusion depth and speed is much higher than the thermal diffusion (right).

5.6. Wearable Energy Supply Devices

As applications of soft bioelectronics expand, demand for more portable/wearable energy storage devices will also continue to increase. Nanomaterials and their hybrids have been actively used in these deformable energy harvesting and storage devices. In particular, the large surface area as well as the soft nature of nanoscale materials provides more reaction sites to generate and/or store energy with high mechanical deformability. These energy devices are conformally mounted on the human body, and can harvest and store energy from daily movements, sunlight, or residual heat, and supply it to the wearable/implantable bioelectronics systems.

Wearable piezoelectric energy harvesting devices have been demonstrated to generate electric power from the mechanical vibrations of daily movements. The elastic piezoelectric nano-composite employing piezoelectric micro-particles (PMN-PT particles; lead magnesium niobate–lead titanate) and MWCNTs, mixed in a silicone rubber, generates electricity under mechanical stresses with stable output voltage and current (**Figure 12**a).[109] Ultra-long Ag NW networks as stretchable electrodes help to efficiently extract generated charges. The triboelectric energy harvesting from contact and separation between textile substrates is another useful power generation in wearable systems.[110] Nanostructured surface of triboelectric generator promotes triboelectrification effect by increasing the effective contact area and friction (Figure 12b).[110] The surface of ZnO NWs vertically grown on the Ag-coated textile substrate is modified by PDMS
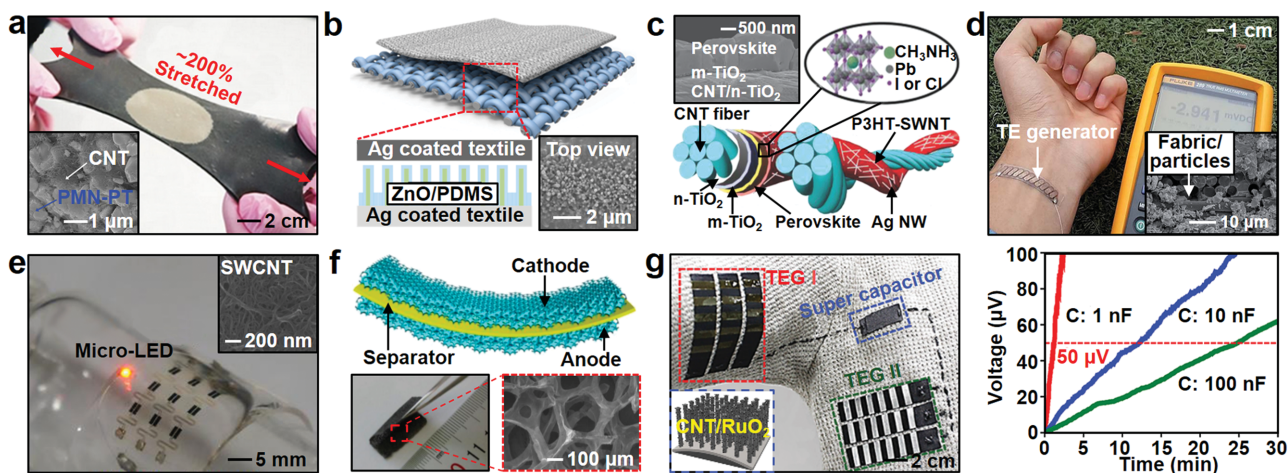
Figure 12. Wearable energy supply devices. a) An optical camera image of a stretchable piezoelectric nanogenerator. The inset shows good dispersion of piezoelectric microparticles and MWCNTs. Reproduced with permission.[109] Copyright 2015, Wiley-VCH. b) A schematic illustration of the wearable triboelectric generator. The inset shows a SEM image of the PDMS-coated ZnO NRs. Reproduced with permission.[110] Copyright 2015, American Chemical Society. c) A schematic illustration of a CNT-fiber-based perovskite solar cell. The SEM image shows cross-sectional view of the solar cell (inset). Reproduced with permission.[111] Copyright 2015, Wiley-VCH. d) An optical camera image of a band-type flexible thermoelectric generator mounted on human skin. Reproduced with permission.[112] Copyright 2014, the Royal Society of Chemistry. e) An optical camera image of a stretchable supercapacitor array. The inset shows a SEM image of the SWCNT random network on a current collector electrode. Reproduced with permission.[113] Copyright 2013, American Chemical Society. f) A schematic illustration of a flexible battery using a 3D interconnected graphene foam (top). An optical camera image on the left bottom inset shows the bent image of the 3D interconnected graphene foam. A SEM image on the right bottom inset shows the magnified view of the graphene foam electrode. Reproduced with permission.[114] Copyright 2012, National Academy of Sciences USA. g) An integrated energy supply system composed of a carbon fabric-based triboelectric generator (TEG) and a SWCNT-based supercapacitor (left). Charging the supercapacitor with various speeds with integrated TEG (right). Reproduced with permission.[39] Copyright 2014, Wiley-VCH.

and contacted with another Ag-coated textile. While there are sustained progresses in this field of energy harvesting technologies, there remain challenges in improving the energy harvesting efficiencies of piezo- and tribo-electric generators, which typically show non-continuous power generation with low currents.

Photovoltaic energy harvesting devices represent another type of power sources with continuous energy generation. To fabricate a solar cell as a wearable form, a functional fabric composed of CNT fibers coated with TiO_2 layers, perovskite, and P3HT/SWCNT/Ag NWs is developed (Figure 12c).[111] This flexible and fiber-shaped solar cell shows stable power generation performances and mechanical reliability under physical deformations, applicable to self-powering wearable energy supply modules. Another continuous power generation device that can be made wearable is thermoelectric devices. The temperature of human body and its temperature difference with ambient air are maintained to be similar (almost constant) due to homeostasis. This temperature difference can be used to generate electricity by using a thermoelectric power generator. One example of a flexible thermoelectric generator uses screen printing of thermoelectric materials on a flexible glass fabric substrate. This thermoelectric generator shows high output power density on human skin (Figure 12d).[112] Protective encapsulating layers are required to help prevent exposure to the toxic effects of thermoelectric materials in wearable applications.

Nanomaterials have large electrochemical surface areas, which can be utilized for energy storage devices. Random networked SWCNTs, for instance, can be used as electrodes in stretchable supercapacitors (Figure 12e).[113] Supercapacitors

designed with serpentine interconnections and fabricated with elastomeric substrates demonstrate stable charge and discharge characteristics under physical deformations. Similarly, nanomaterials with large surface areas and electrochemically active surfaces can be applied for a flexible lithium ion battery. The wearable battery can supply larger amount of energy to bioelectronics systems than the supercapacitor. The 3D graphene foam grown by a chemical vapor deposition process is a good example for electrodes in a wearable battery. The graphene foam is light-weight, flexible and highly porous (≈99.7%), and has very high specific surface area, which are all important advantages (Figure 12f).[114] This flexible lithium ion battery shows high-rate performance, energy density, and electrochemical stability.

In order to implement fully wearable bioelectronics systems, both energy harvesting and energy storage devices are monolithically integrated with other electronics, such as epidermal biosensors. Figure 12g left shows an example of this wearable energy supply system to integrated pressure sensors.[39] Carbon fabric is used as a conducting substrate for triboelectric generators (TEG) and a supercapacitor. Vertically-grown SWCNT on a carbon fabric substrate extends the surface area and ruthenium oxide nanoparticles coated on SWCNT maximize the capacity. The charge accumulation rate in a supercapacitor is dependent on the rubbing frequency of TEGs determined by human activity (right). The stored energy in the supercapacitor is used to operate integrated pressure sensors. These integrated energy harvesting and storage devices[39,115] would enable self-powered operations of wearable and implantable bioelectronics systems.

PROGRESS REPORT

6. Conclusion and Perspectives

Over the past decade, advances in device designs, mechanical analysis, and micro-/nano-fabrication techniques have accelerated development of soft electronics and optoelectronics applications in biomedicine. These electronics have unique mechanical and multifunctional characteristics due in part to advances in hybridized nanomaterials. There are several remaining challenges and opportunities for effective integration of these nanomaterials in soft-bioelectronics. There are many different classes of nanomaterials of varying sizes, dimensions, material properites, and function. Biocompatibility of nanomaterials with long term toxicity analysis is a critical area of future research particularly for the more invasive applications detailed in this report. These challenges are being addressed through novel use of materials, assemblies, surface/interface, and device designs. The development of these new materials and processes will give rise to emerging soft, stretchable bioelectronics, whose paradigm would extend the scope of current diagnostic and therapeutic technologies in health care.

[1] M. Kaltenbrunner, T. Sekitani, J. Reeder, T. Yokota, K. Kuribara, T. Tokuhara, M. Drack, R. Schwodiauer, I. Graz, S. Bauer-Gogonea, S. Bauer, T. Someya, *Nature* **2013**, *499*, 458.

[2] M. Drack, I. Graz, T. Sekitani, T. Someya, M. Kaltenbrunner, S. Bauer, *Adv. Mater.* **2015**, *27*, 34.

[3] D. H. Kim, N. Lu, R. Ma, Y. S. Kim, R. H. Kim, S. Wang, J. Wu, S. M. Won, H. Tao, A. Islam, K. J. Yu, T. I. Kim, R. Chowdhury, M. Ying, L. Xu, M. Li, H. J. Chung, H. Keum, M. McCormick, P. Liu, Y. W. Zhang, F. G. Omenetto, Y. Huang, T. Coleman, J. A. Rogers, *Science* **2011**, *333*, 838.

[4] H. Tao, S. W. Hwang, B. Marelli, B. An, J. E. Moreau, M. Yang, M. A. Brenckle, S. Kim, D. L. Kaplan, J. A. Rogers, F. G. Omenetto, *Proc. Natl. Acad. Sci. USA* **2014**, *111*, 17385.

[5] R. Farra, N. F. Sheppard Jr., L. McCabe, R. M. Neer, J. M. Anderson, J. T. Santini Jr., M. J. Cima, R. Langer, *Sci. Transl. Med.* **2012**, *4*, 122ra21.

[6] S.-W. Hwang, H. Tao, D.-H. Kim, H. Cheng, J.-K. Song, E. Rill, M. A. Brenckle, B. Panilaitis, S. M. Won, Y.-S. Kim, Y. M. Song, K. J. Yu, A. Ameen, R. Li, Y. Su, M. Yang, D. L. Kaplan, M. R. Zakin, M. J. Slepian, Y. Huang, F. G. Omenetto, J. A. Rogers, *Science* **2012**, *337*, 1640.

[7] D. H. Kim, J. Viventi, J. J. Amsden, J. Xiao, L. Vigeland, Y. S. Kim, J. A. Blanco, B. Panilaitis, E. S. Frechette, D. Contreras, D. L. Kaplan, F. G. Omenetto, Y. Huang, K. C. Hwang, M. R. Zakin, B. Litt, J. A. Rogers, *Nat. Mater.* **2010**, *9*, 511.

[8] T. Yamada, Y. Hayamizu, Y. Yamamoto, Y. Yomogida, A. Izadi-Najafabadi, D. N. Futaba, K. Hata, *Nat. Nanotechnol.* **2011**, *6*, 296.

[9] J. J. S. Norton, D. S. Lee, J. W. Lee, W. Lee, O. Kwon, P. Won, S.-Y. Jung, H. Cheng, J.-W. Jeong, A. Akce, S. Umunna, I. Na, Y. H. Kwon, X.-Q. Wang, Z. Liu, U. Paik, Y. Huang, T. Bretl, W.-H. Yeo, J. A. Rogers, *Proc. Natl. Acad. Sci. USA* **2015**, *112*, 3920.

[10] W. H. Yeo, Y. S. Kim, J. Lee, A. Ameen, L. Shi, M. Li, S. Wang, R. Ma, S. H. Jin, Z. Kang, Y. Huang, J. A. Rogers, *Adv. Mater.* **2013**, *25*, 2773.

[11] S. Xu, Y. Zhang, L. Jia, K. E. Mathewson, K. I. Jang, J. Kim, H. Fu, X. Huang, P. Chava, R. Wang, S. Bhole, L. Wang, Y. J. Na, Y. Guan, M. Flavin, Z. Han, Y. Huang, J. A. Rogers, *Science* **2014**, *344*, 70.

[12] J. W. Jeong, W. H. Yeo, A. Akhtar, J. J. Norton, Y. J. Kwack, S. Li, S. Y. Jung, Y. Su, W. Lee, J. Xia, H. Cheng, Y. Huang, W. S. Choi, T. Bretl, J. A. Rogers, *Adv. Mater.* **2013**, *25*, 6839.

[13] G. Schwartz, B. C. Tee, J. Mei, A. L. Appleton, H. Kim do, H. Wang, Z. Bao, *Nat. Commun.* **2013**, *4*, 1859.

[14] R. C. Webb, A. P. Bonifas, A. Behnaz, Y. Zhang, K. J. Yu, H. Cheng, M. Shi, Z. Bian, Z. Liu, Y. S. Kim, W. H. Yeo, J. S. Park, J. Song, Y. Li, Y. Huang, A. M. Gorbach, J. A. Rogers, *Nat. Mater.* **2013**, *12*, 938.

[15] M. Park, K. Do, J. Kim, D. Son, J. H. Koo, J. Park, J. K. Song, J. H. Kim, M. Lee, T. Hyeon, D. H. Kim, *Adv. Healthcare Mater.* **2015**, *4*, 992.

[16] D. J. Lipomi, M. Vosgueritchian, B. C. Tee, S. L. Hellstrom, J. A. Lee, C. H. Fox, Z. Bao, *Nat. Nanotechnol.* **2011**, *6*, 788.

[17] A. J. Bandodkar, V. W. Hung, W. Jia, G. Valdes-Ramirez, J. R. Windmiller, A. G. Martinez, J. Ramirez, G. Chan, K. Kerman, J. Wang, *Analyst* **2013**, *138*, 123.

[18] A. J. Bandodkar, W. Jia, C. Yardimci, X. Wang, J. Ramirez, J. Wang, *Anal. Chem.* **2015**, *87*, 394.

[19] S. Nattel, *Nature* **2002**, *415*, 219.

[20] M. C. Sanguinetti, M. Tristani-Firouzi, *Nature* **2006**, *440*, 463.

[21] C. A. Massey, L. P. Sowers, B. J. Dlouhy, G. B. Richerson, *Nat. Rev. Neurol.* **2014**, *10*, 271.

[22] J. A. Rogers, M. G. Lagally, R. G. Nuzzo, *Nature* **2011**, *477*, 45.

[23] P. Lee, J. Lee, H. Lee, J. Yeo, S. Hong, K. H. Nam, D. Lee, S. S. Lee, S. H. Ko, *Adv. Mater.* **2012**, *24*, 3326.

[24] F. Schwierz, *Nat. Nanotechnol.* **2010**, *5*, 487.

[25] Y. Shirasaki, G. J. Supran, M. G. Bawendi, V. Bulovći, *Nat. Photonics* **2012**, *7*, 13.

[26] F. Bonaccorso, Z. Sun, T. Hasan, A. C. Ferrari, *Nat. Photonics* **2010**, *4*, 611.

[27] A. L. Mohana Reddy, S. R. Gowda, M. M. Shaijumon, P. M. Ajayan, *Adv. Mater.* **2012**, *24*, 5045.

[28] H. C. Ko, M. P. Stoykovich, J. Song, V. Malyarchuk, W. M. Choi, C. J. Yu, J. B. Geddes 3rd, J. Xiao, S. Wang, Y. Huang, J. A. Rogers, *Nature* **2008**, *454*, 748.

[29] J. Kim, M. Lee, H. J. Shim, R. Ghaffari, H. R. Cho, D. Son, Y. H. Jung, M. Soh, C. Choi, S. Jung, K. Chu, D. Jeon, S. T. Lee, J. H. Kim, S. H. Choi, T. Hyeon, D. H. Kim, *Nat. Commun.* **2014**, *5*, 5747.

[30] T. I. Kim, J. G. McCall, Y. H. Jung, X. Huang, E. R. Siuda, Y. Li, J. Song, Y. M. Song, H. A. Pao, R. H. Kim, C. Lu, S. D. Lee, I. S. Song, G. Shin, R. Al-Hasani, S. Kim, M. P. Tan, Y. Huang, F. G. Omenetto, J. A. Rogers, M. R. Bruchas, *Science* **2013**, *340*, 211.

[31] D. H. Kim, N. Lu, R. Ghaffari, Y. S. Kim, S. P. Lee, L. Xu, J. Wu, R. H. Kim, J. Song, Z. Liu, J. Viventi, B. de Graff, B. Elolampi, M. Mansour, M. J. Slepian, S. Hwang, J. D. Moss, S. M. Won, Y. Huang, B. Litt, J. A. Rogers, *Nat. Mater.* **2011**, *10*, 316.

[32] D.-H. Kim, R. Ghaffari, N. Lu, S. Wang, S. P. Lee, H. Keum, R. D'Angelo, L. Klinker, Y. Su, C. Lu, Y.-S. Kim, A. Ameen, Y. Li, Y. Zhang, B. de Graff, Y.-Y. Hsu, Z. Liu, J. Ruskin, L. Xu, C. Lu, F. G. Omenetto, Y. Huang, M. Mansour, M. J. Slepian, J. A. Rogers, *Proc. Natl. Acad. Sci. USA* **2012**, *109*, 19910.

[33] D. Son, J. Lee, D. J. Lee, R. Ghaffari, S. Yun, S. J. Kim, J. E. Lee, H. R. Cho, S. Yoon, S. Yang, S. Lee, S. Qiao, D. Ling, S. Shin, J.-K. Song, J. Kim, T. Kim, H. Lee, J. Kim, M. Soh, N. Lee, C. S. Hwang, S. Nam, N. Lu, T. Hyeon, S. H. Choi, D.-H. Kim, *ACS Nano* **2015**, *9*, 5937.

[34] D. Son, J. Lee, S. Qiao, R. Ghaffari, J. Kim, J. E. Lee, C. Song, S. J. Kim, D. J. Lee, S. W. Jun, S. Yang, M. Park, J. Shin, K. Do, M. Lee, K. Kang, C. S. Hwang, N. Lu, T. Hyeon, D. H. Kim, *Nat. Nanotechnol.* **2014**, *9*, 397.

[35] M. K. Choi, O. K. Park, C. Choi, S. Qiao, R. Ghaffari, J. Kim, D. J. Lee, M. Kim, W. Hyun, S. J. Kim, H. J. Hwang, S. H. Kwon, T. Hyeon, N. Lu, D. H. Kim, *Adv. Healthcare Mater.* **2015**, DOI: 10.1002/adhm.201500285.

[36] J. Park, K. An, Y. Hwang, J. G. Park, H. J. Noh, J. Y. Kim, J. H. Park, N. M. Hwang, T. Hyeon, *Nat. Mater.* **2004**, *3*, 891.

[37] E. Roduner, *Chem. Soc. Rev.* **2006**, *35*, 583.

[38] A. M. Munshi, D. L. Dheeraj, V. T. Fauske, D. C. Kim, J. Huh, J. F. Reinertsen, L. Ahtapodov, K. D. Lee, B. Heidari, A. T. van Helvoort, B. O. Fimland, H. Weman, *Nano Lett.* **2014**, *14*, 960.

[39] S. Jung, J. Lee, T. Hyeon, M. Lee, D. H. Kim, *Adv. Mater.* **2014**, *26*, 6329.

[40] S. Kim, Y. Su, A. Mihi, S. Lee, Z. Liu, T. K. Bhandakkar, J. Wu, J. B. Geddes 3rd, H. T. Johnson, Y. Zhang, J. K. Park, P. V. Braun, Y. Huang, J. A. Rogers, *Small* **2012**, *8*, 901.

[41] S. Paul, C. Pearson, A. Molloy, M. A. Cousins, M. Green, S. Kolliopoulou, P. Dimitrakis, P. Normand, D. Tsoukalas, M. C. Petty, *Nano Lett.* **2003**, *3*, 533.

[42] Z. Fan, J. C. Ho, Z. A. Jacobson, R. Yerushalmi, R. L. Alley, H. Razavi, A. Javey, *Nano Lett.* **2008**, *8*, 20.

[43] S. Kim, J. Wu, A. Carlson, S. H. Jin, A. Kovalsky, P. Glass, Z. Liu, N. Ahmed, S. L. Elgan, W. Chen, P. M. Ferreira, M. Sitti, Y. Huang, J. A. Rogers, *Proc. Natl. Acad. Sci. USA* **2010**, *107*, 17095.

[44] M. Kaltenbrunner, M. S. White, E. D. Glowacki, T. Sekitani, T. Someya, N. S. Sariciftci, S. Bauer, *Nat. Commun.* **2012**, *3*, 770.

[45] D.-H. Kim, J.-H. Ahn, W. M. Choi, H.-S. Kim, T.-H. Kim, J. Song, Y. Y. Huang, Z. Liu, C. Lu, J. A. Rogers, *Science* **2008**, *320*, 507.

[46] J. A. Fan, W. H. Yeo, Y. Su, Y. Hattori, W. Lee, S. Y. Jung, Y. Zhang, Z. Liu, H. Cheng, L. Falgout, M. Bajema, T. Coleman, D. Gregoire, R. J. Larsen, Y. Huang, J. A. Rogers, *Nat. Commun.* **2014**, *5*, 3266.

[47] L. D. Landau, E. M. Lifshitz, *Theory of Elasticity*, Vol. *7*, Butterworth-Heinemann, Oxford, UK, **1986**, p. 42.

[48] D.-H. Kim, W. M. Choi, J.-H. Ahn, H.-S. Kim, J. Song, Y. Huang, Z. Liu, C. Lu, C. G. Koh, J. A. Rogers, *Appl. Phys. Lett.* **2008**, *93*.

[49] C. Pang, G. Y. Lee, T. I. Kim, S. M. Kim, H. N. Kim, S. H. Ahn, K. Y. Suh, *Nat. Mater.* **2012**, *11*, 795.

[50] C. Pang, J. H. Koo, A. Nguyen, J. M. Caves, M. G. Kim, A. Chortos, K. Kim, P. J. Wang, J. B. Tok, Z. Bao, *Adv. Mater.* **2015**, *27*, 634.

[51] S. C. Mannsfeld, B. C. Tee, R. M. Stoltenberg, C. V. Chen, S. Barman, B. V. Muir, A. N. Sokolov, C. Reese, Z. Bao, *Nat. Mater.* **2010**, *9*, 859.

[52] S. Lee, Y. Inoue, D. Kim, A. Reuveny, K. Kuribara, T. Yokota, J. Reeder, M. Sekino, T. Sekitani, Y. Abe, T. Someya, *Nat. Commun.* **2014**, *5*, 5898.

[53] K. I. Jang, H. U. Chung, S. Xu, C. H. Lee, H. Luan, J. Jeong, H. Cheng, G. T. Kim, S. Y. Han, J. W. Lee, J. Kim, M. Cho, F. Miao, Y. Yang, H. N. Jung, M. Flavin, H. Liu, G. W. Kong, K. J. Yu, S. I. Rhee, J. Chung, B. Kim, J. W. Kwak, M. H. Yun, J. Y. Kim, Y. M. Song, U. Paik, Y. Zhang, Y. Huang, J. A. Rogers, *Nat. Commun.* **2015**, *6*, 6566.

[54] C. Dagdeviren, Y. Shi, P. Joe, R. Ghaffari, G. Balooch, K. Usgaonkar, O. Gur, P. L. Tran, J. R. Crosby, M. Meyer, Y. Su, R. Chad Webb, A. S. Tedesco, M. J. Slepian, Y. Huang, J. A. Rogers, *Nat. Mater.* **2015**, *14*, 728.

[55] Y. Hattori, L. Falgout, W. Lee, S. Y. Jung, E. Poon, J. W. Lee, I. Na, A. Geisler, D. Sadhwani, Y. Zhang, Y. Su, X. Wang, Z. Liu, J. Xia, H. Cheng, R. C. Webb, A. P. Bonifas, P. Won, J. W. Jeong, K. I. Jang, Y. M. Song, B. Nardone, M. Nodzenski, J. A. Fan,

[56] Y. Huang, D. P. West, A. S. Paller, M. Alam, W. H. Yeo, J. A. Rogers, *Adv. Healthcare Mater.* **2014**, *3*, 1597.

[56] S. Yang, Y. C. Chen, L. Nicolini, P. Pasupathy, J. Sacks, S. Becky, R. Yang, S. Daniel, Y. F. Chang, P. Wang, D. Schnyer, D. Neikirk, N. Lu, *Adv. Mater.* **2015**, *27*, 6423.

[57] L. Xu, S. R. Gutbrod, A. P. Bonifas, Y. Su, M. S. Sulkin, N. Lu, H. J. Chung, K. I. Jang, Z. Liu, M. Ying, C. Lu, R. C. Webb, J. S. Kim, J. I. Laughner, H. Cheng, Y. Liu, A. Ameen, J. W. Jeong, G. T. Kim, Y. Huang, I. R. Efimov, J. A. Rogers, *Nat. Commun.* **2014**, *5*, 3329.

[58] L. Xu, S. R. Gutbrod, Y. Ma, A. Petrossians, Y. Liu, R. C. Webb, J. A. Fan, Z. Yang, R. Xu, J. J. Whalen , 3rd, J. D. Weiland, Y. Huang, I. R. Efimov, J. A. Rogers, *Adv. Mater.* **2015**, *27*, 1731.

[59] J. Viventi, D. H. Kim, L. Vigeland, E. S. Frechette, J. A. Blanco, Y. S. Kim, A. E. Avrin, V. R. Tiruvadi, S. W. Hwang, A. C. Vanleer, D. F. Wulsin, K. Davis, C. E. Gelber, L. Palmer, J. Van der Spiegel, J. Wu, J. Xiao, Y. Huang, D. Contreras, J. A. Rogers, B. Litt, *Nat. Neurosci.* **2011**, *14*, 1599.

[60] D. Khodagholy, J. N. Gelinas, T. Thesen, W. Doyle, O. Devinsky, G. G. Malliaras, G. Buzsaki, *Nat. Neurosci.* **2015**, *18*, 310.

[61] D. Qi, Z. Liu, M. Yu, Y. Liu, Y. Tang, J. Lv, Y. Li, J. Wei, B. Liedberg, Z. Yu, X. Chen, *Adv. Mater.* **2015**, *27*, 3145.

[62] I. R. Minev, P. Musienko, A. Hirsch, Q. Barraud, N. Wenger, E. M. Moraud, J. Gandar, M. Capogrosso, T. Milekovic, L. Asboth, R. F. Torres, N. Vachicouras, Q. Liu, N. Pavlova, S. Duis, A. Larmagnac, J. Voeroes, S. Micera, Z. Suo, G. Courtine, S. P. Lacour, *Science* **2015**, *347*, 159.

[63] D. Khodagholy, T. Doublet, M. Gurfinkel, P. Quilichini, E. Ismailova, P. Leleux, T. Herve, S. Sanaur, C. Bernard, G. G. Malliaras, *Adv. Mater.* **2011**, *23*, H268.

[64] M. Sessolo, D. Khodagholy, J. Rivnay, F. Maddalena, M. Gleyzes, E. Steidl, B. Buisson, G. G. Malliaras, *Adv. Mater.* **2013**, *25*, 2135.

[65] M. Ramuz, B. C. Tee, J. B. Tok, Z. Bao, *Adv. Mater.* **2012**, *24*, 3223.

[66] G. J. Chader, J. Weiland, M. S. Humayun, in *Neurotherapy: Progress in Restorative Neuroscience and Neurology*, Vol. *175* (Eds: J. Verhaagen, E. M. Hol, I. Huitenga, J. Wijnholds, A. B. Bergen, G. J. Boer, D. F. Swaab), Elsevier, Amsterdam, Netherlands, **2009**, 317–331.

[67] K. Deisseroth, *Nat. Methods* **2011**, *8*, 26.

[68] R. H. Kim, D. H. Kim, J. Xiao, B. H. Kim, S. I. Park, B. Panilaitis, R. Ghaffari, J. Yao, M. Li, Z. Liu, V. Malyarchuk, D. G. Kim, A. P. Le, R. G. Nuzzo, D. L. Kaplan, F. G. Omenetto, Y. Huang, Z. Kang, J. A. Rogers, *Nat. Mater.* **2010**, *9*, 929.

[69] Y. M. Song, Y. Xie, V. Malyarchuk, J. Xiao, I. Jung, K. J. Choi, Z. Liu, H. Park, C. Lu, R. H. Kim, R. Li, K. B. Crozier, Y. Huang, J. A. Rogers, *Nature* **2013**, *497*, 95.

[70] D. J. Lipomi, B. C. Tee, M. Vosgueritchian, Z. Bao, *Adv. Mater.* **2011**, *23*, 1771.

[71] S. Xu, Y. Zhang, J. Cho, J. Lee, X. Huang, L. Jia, J. A. Fan, Y. Su, J. Su, H. Zhang, H. Cheng, B. Lu, C. Yu, C. Chuang, T. I. Kim, T. Song, K. Shigeta, S. Kang, C. Dagdeviren, I. Petrov, P. V. Braun, Y. Huang, U. Paik, J. A. Rogers, *Nat. Commun.* **2013**, *4*, 1543.

[72] J. Kim, A. Banks, Z. Xie, S. Y. Heo, P. Gutruf, J. W. Lee, S. Xu, K.-I. Jang, F. Liu, G. Brown, J. Choi, J. H. Kim, X. Feng, Y. Huang, U. Paik, J. A. Rogers, *Adv. Funct. Mater.* **2015**, *25*, 4761.

[73] J. Kim, A. Banks, H. Cheng, Z. Xie, S. Xu, K. I. Jang, J. W. Lee, Z. Liu, P. Gutruf, X. Huang, P. Wei, F. Liu, K. Li, M. Dalal, R. Ghaffari, X. Feng, Y. Huang, S. Gupta, U. Paik, J. A. Rogers, *Small* **2015**, *11*, 906.

[74] X. Huang, Y. Liu, K. Chen, W. J. Shin, C. J. Lu, G. W. Kong, D. Patnaik, S. H. Lee, J. F. Cortes, J. A. Rogers, *Small* **2014**, *10*, 3083.

[75] N. Lu, C. Lu, S. Yang, J. Rogers, *Adv. Funct. Mater.* **2012**, *22*, 4044.

[76] F. Xu, Y. Zhu, *Adv. Mater.* **2012**, *24*, 5117.

[77] T. Sekitani, Y. Noguchi, K. Hata, T. Fukushima, T. Aida, T. Someya, *Science* **2008**, *321*, 1468.

[78] S. Jung, J. H. Kim, J. Kim, S. Choi, J. Lee, I. Park, T. Hyeon, D. H. Kim, *Adv. Mater.* **2014**, *26*, 4825.

[79] S. Lim, D. Son, J. Kim, Y. B. Lee, J.-K. Song, S. Choi, D. J. Lee, J. H. Kim, M. Lee, T. Hyeon, D.-H. Kim, *Adv. Funct. Mater.* **2015**, *25*, 375.

[80] M. Ha, S. Lim, J. Park, D. S. Um, Y. Lee, H. Ko, *Adv. Funct. Mater.* **2015**, *25*, 2841.

[81] J. Park, Y. Lee, J. Hong, M. Ha, Y. D. Jung, H. Lim, S. Y. Kim, H. Ko, *ACS Nano* **2014**, *8*, 4689.

[82] S. Xu, Y. Qin, C. Xu, Y. Wei, R. Yang, Z. L. Wang, *Nat. Nanotechnol.* **2010**, *5*, 366.

[83] M. Lee, C. Y. Chen, S. Wang, S. N. Cha, Y. J. Park, J. M. Kim, L. J. Chou, Z. L. Wang, *Adv. Mater.* **2012**, *24*, 1759.

[84] K. Takei, T. Takahashi, J. C. Ho, H. Ko, A. G. Gillies, P. W. Leu, R. S. Fearing, A. Javey, *Nat. Mater.* **2010**, *9*, 821.

[85] Z. Fan, J. C. Ho, T. Takahashi, R. Yerushalmi, K. Takei, A. C. Ford, Y.-L. Chueh, A. Javey, *Adv. Mater.* **2009**, *21*, 3730.

[86] C. Wang, D. Hwang, Z. Yu, K. Takei, J. Park, T. Chen, B. Ma, A. Javey, *Nat. Mater.* **2013**, *12*, 899.

[87] L. Gao, Y. Zhang, V. Malyarchuk, L. Jia, K. I. Jang, R. C. Webb, H. Fu, Y. Shi, G. Zhou, L. Shi, D. Shah, X. Huang, B. Xu, C. Yu, Y. Huang, J. A. Rogers, *Nat. Commun.* **2014**, *5*, 4938.

[88] M. K. Choi, J. Yang, K. Kang, D. C. Kim, C. Choi, C. Park, S. J. Kim, S. I. Chae, T. H. Kim, J. H. Kim, T. Hyeon, D. H. Kim, *Nat. Commun.* **2015**, *6*, 7149.

[89] M. K. Choi, I. Park, D. C. Kim, E. Joh, O. K. Park, J. Kim, M. Kim, C. Choi, J. Yang, K. W. Cho, J.-H. Hwang, J.-M. Nam, T. Hyeon, J. H. Kim, D.-H. Kim, *Adv. Funct. Mater.* **2015**, *25*, 7109.

[90] T.-H. Kim, K.-S. Cho, E. K. Lee, S. J. Lee, J. Chae, J. W. Kim, D. H. Kim, J.-Y. Kwon, G. Amaratunga, S. Y. Lee, B. L. Choi, Y. Kuk, J. M. Kim, K. Kim, *Nat. Photonics* **2011**, *5*, 176.

[91] J. M. Caruge, J. E. Halpert, V. Wood, V. Bulović, M. G. Bawendi, *Nat. Photonics* **2008**, *2*, 247.

[92] F. Vitale, S. R. Summerson, B. Aazhang, C. Kemere, M. Pasquali, *ACS Nano* **2015**, *9*, 4465.

[93] H. Zhang, J. Shih, J. Zhu, N. A. Kotov, *Nano Lett.* **2012**, *12*, 3391.

[94] S. J. Kim, H. R. Cho, K. W. Cho, S. Qiao, J. S. Rhim, M. Soh, T. Kim, M. K. Choi, C. Choi, I. Park, N. S. Hwang, T. Hyeon, S. H. Choi, N. Lu, D.-H. Kim, *ACS Nano* **2015**, *9*, 2677.

[95] B. Tian, J. Liu, T. Dvir, L. Jin, J. H. Tsui, Q. Qing, Z. Suo, R. Langer, D. S. Kohane, C. M. Lieber, *Nat. Mater.* **2012**, *11*, 986.

[96] H. Lee, Y. Lee, C. Song, H. R. Cho, R. Ghaffari, T. K. Choi, K. H. Kim, Y. B. Lee, D. Ling, H. Lee, S. J. Yu, S. H. Choi, T. Hyeon, D.-H. Kim, *Nat. Commun.* **2015**, *6*, 10059.

[97] S. Y. Park, J. Park, S. H. Sim, M. G. Sung, K. S. Kim, B. H. Hong, S. Hong, *Adv. Mater.* **2011**, *23*, H263.

[98] J. Liu, T. M. Fu, Z. Cheng, G. Hong, T. Zhou, L. Jin, M. Duvvuri, Z. Jiang, P. Kruskal, C. Xie, Z. Suo, Y. Fang, C. M. Lieber, *Nat. Nanotechnol.* **2015**, *10*, 629.

[99] D. Son, J. H. Koo, J.-K. Song, J. Kim, M. Lee, H. J. Shim, M. Park, M. Lee, J. H. Kim, D.-H. Kim, *ACS Nano* **2015**, *9*, 5585.

[100] S. Bertolazzi, D. Krasnozhon, A. Kis, *ACS Nano* **2013**, *7*, 3246.

[101] A. A. Bessonov, M. N. Kirikova, D. I. Petukhov, M. Allen, T. Ryhanen, M. J. Bailey, *Nat. Mater.* **2015**, *14*, 199.

[102] Y. Ko, H. Baek, Y. Kim, M. Yoon, J. Cho, *ACS Nano* **2013**, *7*, 143.

[103] S. T. Han, Y. Zhou, C. Wang, L. He, W. Zhang, V. A. Roy, *Adv. Mater.* **2013**, *25*, 872.

[104] S. Choi, J. Park, W. Hyun, J. Kim, J. Kim, Y. B. Lee, C. Song, H. J. Hwang, J. H. Kim, T. Hyeon, D.-H. Kim, *ACS Nano* **2015**, *9*, 6626.

[105] M. S. Lee, K. Lee, S. Y. Kim, H. Lee, J. Park, K. H. Choi, H. K. Kim, D. G. Kim, D. Y. Lee, S. Nam, J. U. Park, *Nano Lett.* **2013**, *13*, 2814.

[106] J. Kim, M. S. Lee, S. Jeon, M. Kim, S. Kim, K. Kim, F. Bien, S. Y. Hong, J. U. Park, *Adv. Mater.* **2015**, *27*, 3292.

[107] M. Zaric, O. Lyubomska, O. Touzelet, C. Poux, S. Al-Zahrani, F. Fay, L. Wallace, D. Terhorst, B. Malissen, S. Henri, U. F. Power, C. J. Scott, R. F. Donnelly, A. Kissenpfennig, *ACS Nano* **2013**, *7*, 2042.

[108] J. Yu, Y. Zhang, Y. Ye, R. DiSanto, W. Sun, D. Ranson, F. S. Ligler, J. B. Buse, Z. Gu, *Proc. Natl. Acad. Sci. USA* **2015**, *112*, 8260.

[109] C. K. Jeong, J. Lee, S. Han, J. Ryu, G. T. Hwang, D. Y. Park, J. H. Park, S. S. Lee, M. Byun, S. H. Ko, K. J. Lee, *Adv. Mater.* **2015**, *27*, 2866.

[110] W. Seung, M. K. Gupta, K. Y. Lee, K.-S. Shin, J.-H. Lee, T. Y. Kim, S. Kim, J. Lin, J. H. Kim, S.-W. Kim, *ACS Nano* **2015**, *9*, 3501.

[111] R. Li, X. Xiang, X. Tong, J. Zou, Q. Li, *Adv. Mater.* **2015**, *27*, 3831.

[112] S. J. Kim, J. H. We, B. J. Cho, *Energy Environ. Sci.* **2014**, *7*, 1959.

[113] D. Kim, G. Shin, Y. J. Kang, W. Kim, J. S. Ha, *ACS Nano* **2013**, *7*, 7975.

[114] N. Li, Z. P. Chen, W. C. Ren, F. Li, H. M. Cheng, *Proc. Natl. Acad. Sci. USA* **2012**, *109*, 17360.

[115] S. Jung, S. Hong, J. Kim, S. Lee, T. Hyeon, M. Lee, D.-H. Kim, *Sci. Rep.* **2015**, *5*, 17081.